

Residential Energy Storage Management with Bidirectional Energy Control

Tianyi Li, and Min Dong, *Senior Member, IEEE*

Abstract—We consider the residential energy storage management system with integrated renewable generation and the availability of bidirectional energy flow from and to the grid through buying and selling. We propose a real-time bidirectional energy control algorithm, aiming to minimize the net system cost from energy buying and selling as well as battery deterioration and storage inefficiency within a given time period, subject to the battery operational constraints and energy buying and selling constraints. We formulate the problem as a stochastic control optimization problem. We then modify and transform this difficult problem into one that enables us to develop the real-time energy control algorithm through Lyapunov optimization. Our developed algorithm is applicable to arbitrary and unknown statistics of renewable generation, load, and electricity prices. It provides a simple closed-form control solution based on only current system states, and requires a minimum complexity for real-time implementation. Furthermore, the solution structure reveals how the battery energy level and energy prices affect the energy flow direction and storage decision. The proposed algorithm possesses a bounded performance guarantee to that of the optimal non-causal T -slot look-ahead control policy. Simulation shows the effectiveness of our proposed algorithm as compared with alternative real-time and non-causal algorithms, and demonstrates the effect of selling-to-buying price ratio and battery inefficiency on the storage behavior and system cost.

Index Terms—Energy Storage, renewable generation, energy selling, home energy management, Lyapunov optimization, real-time control

I. INTRODUCTION

Energy storage and renewable energy integration are considered key solutions for future power grid infrastructure and services to meet the fast rising energy demand and maintain energy sustainability [1], [2]. For the grid operator, energy storage can be exploited to shift energy across time to meet the demand and counter the fluctuation of intermittent renewable generation to improve grid reliability [2]–[7]. For the electricity customer, local energy storage can provide means for energy management to control energy flow in response to the demand-side management signal and to reduce electricity cost. For example, dynamic pricing is one of main demand-side management techniques to relieve grid congestion [8], [9]. Its effectiveness relies on the customer-side energy management solution to effectively control energy flow and demand in

response to the price change. With local renewable generation and energy storage introduced to residential and commercial customers, there are potentially greater flexibility in energy control to respond to the dynamic pricing and demand fluctuation, as well as maximally harness the energy from renewable source to reduce electricity bills [10]–[15].

With more local renewable generation at customers available, the utility retailer now allows customers to sell energy back to the utility at a price dynamically controlled by the utility in an attempt to harness energy from distributed renewable generation at customers and further improve stability and reliability [16]. This means both renewable generation and previously stored energy, either bought from the grid or harnessed from the renewable source can be sold for profit by the customer. The ability to sell energy back to the grid enables bidirectional energy flow between the energy storage system and the grid. This also gives the customer a greater control capability to manage energy storage and usage based on the dynamic pricing for both buying and selling. The repayment provides return for the storage investment and further reduce the net cost at the customer. An intelligent energy management solution exploring these features to effectively manage storage and control the energy flow, especially at a real-time manner, is crucially needed to maximize the benefits.

Developing an effective energy management system faces many challenges. For the energy storage system itself, the renewable source is intermittent and random, and its statistical characteristics over each day are often inheritably time-varying, making it difficult to predict. The benefit of storage, either for electricity supply or for energy selling back, also comes at the cost of battery operation that should not be neglected. The bidirectional energy flow between the energy storage system and the grid under dynamic pricing complicates the energy control of the system when facing future uncertainty, and creates more challenges. More control decisions need to be made for energy flows among storage battery, the grid, the renewable generation, and the load. The potential profit from energy selling under the unpredictable pricing complicates the control decisions in terms of when and how much to sell, store, or use. Moreover, the battery capacity limitation further makes the control decisions coupled over time and difficult to optimize. In this paper, we aim to develop a real-time energy control solution that addresses these challenges and effectively reduces the net system cost at minimum required knowledge of unpredictable system dynamics.

This work was supported by the National Sciences and Engineering Research Council of Canada under Discovery Grant RGPIN-2014-05181.

Tianyi Li was with Department of Electrical, Computer and Software Engineering, University of Ontario Institute of Technology, Oshawa, Ontario L1H 7K4, Canada. He is now with Huawei Technologies Co., Ltd, Markham, Ontario L3R 5A4, Canada (email: lty616@hotmail.com).

Min Dong is with Department of Electrical, Computer and Software Engineering, University of Ontario Institute of Technology, Oshawa, Ontario L1H 7K4, Canada (email: min.dong@uoit.ca).

A. Related Works

Energy storage has been considered at the power grid operator or aggregator to combat the fluctuation of renewable generation, with many works in literature on storage control and assessment of its role in renewable generation [2], for power balancing with fixed load [3], [4] or flexible load control [6], [7], and for phase balancing [5]. Residential energy storage systems to reduce electricity cost have been considered without renewable [17] and with renewable integration [10]–[13], [18]–[24]. Only energy buying was considered in these works. Among them, off-line storage control strategies for dynamics systems are proposed [10], [11], [18], where combined strategies of load prediction and day-ahead scheduling on respective large and small timescales are proposed. The knowledge of load statistics and renewable generation are known ahead of time, while no battery operational cost are considered.

Real-time energy storage management amid unknown system dynamics is much more challenging. Assuming known distributions of system dynamics (*e.g.*, load, renewable generation, and prices), the storage control problem is formulated as a Markov Decision Process (MDP) and solved numerically using Dynamic Programming [14], [18]. However, this method suffers from high computational complexity to be implementable for practical systems. In addition, due to unpredictable nature of system dynamics, the required statistics are difficult to acquire or predict in practice. Without the statistical knowledge of system dynamics, Lyapunov optimization technique [25] has been employed to develop real-time control strategies in [12], [13], [19]–[22]. For independent and identically distributed or stationary system dynamics (pricing, renewable, and load), energy control algorithms are proposed in [19], [20] without considering battery operational cost, and in [21] with battery charging and discharging operational cost considered. All the above works aim to minimize the long-term average system cost. A real-time energy control algorithm to minimize the system cost within a finite time period is designed in [12] for arbitrary system dynamics. Furthermore, joint storage control and flexible load scheduling is considered in [13] where the closed-form sequential solution was developed to minimize the system cost while meeting the load deadlines.

The idea of energy selling back or trading is considered in [26]–[28], where [26], [27] focus on demand-side management via pricing schemes using game approaches for load scheduling among customers, and [28] considers a microgrid operation and supply. In addition, although not explicitly modeled, the system considered in [24] can be generalized to include energy selling under a simplified model, provided that buying and selling prices are constrained such that the overall cost function is still convex. All these works consider the grid level operation and the cost associated with it, and use a simple battery storage model without considering degradation or operational cost. Since the consumers may prefer a cost saving management solution in a customer-defined time period, and system dynamics may not be stationary, it is important to provide a cost-minimizing solution to meet such need. To the best of our knowledge, there is no such

existing bidirectional energy management solution with energy selling-back capability. In addition, most existing works ignore battery inefficiency in charging and discharging, which results in energy loss that affects the storage behaviors and should be taken into account in the energy storage control design.

B. Contributions

In this paper, we consider a residential energy storage management system with integrated renewable generation and the availability of bidirectional energy flow from and to the grid through buying and selling. We develop a real-time bidirectional energy control algorithm, aiming to minimize the net system cost in a finite time period, subject to the battery operational constraints and energy buying and selling constraints. In considering the system cost, we include the energy storage cost by carefully modeling both battery operational cost and the inefficiency associated with charging/discharging activities. The system dynamics, including renewable generation, buying/selling electricity price, and the customer load, can have arbitrary distributions which may not be stationary, and are unknown to us.

We formulate the net system cost minimization as a stochastic optimization problem over a finite time horizon. The interaction of storage, renewable, and the grid as well as the cost associated with energy buying/selling and battery operation for storage complicate the energy control decision making and optimization over time. To tackle this difficult problem, we use special techniques to modify and transform the original problem into one that we are able to apply Lyapunov optimization to develop a real-time algorithm for the control solution. Our developed real-time algorithm provides a simple closed-form energy control solution, which only relies on the current battery energy level, pricing, load, and renewable generation. It has a minimum complexity for real-time implementation. In addition, the closed-form expression reveals how the battery energy level and prices affect the decisions of energy buying and selling, storage and usage of the battery, and the priority order for storing or selling energy from multiple energy sources. Through analysis, we show that the performance of our proposed real-time algorithm is within a bounded gap to that of the optimal T -slot look-ahead solution which has full system information available ahead of time. The algorithm is also shown to be asymptotically optimal as the battery capacity and the time duration go to infinity. Simulation results demonstrate the effectiveness of our proposed algorithm as compared with alternative real-time or non-causal control solutions. Furthermore, we provide simulation studies to understand the effects of bidirectional energy control, the selling and buying price ratio, and battery efficiency on the energy storage behavior and the system cost.

C. Organization and Notations

The rest of this paper is organized as follows. In Section II, we describe the bidirectional energy storage and management system model. In Section III, we formulate the stochastic energy control optimization problem and develop an approach to transform it for the real-time control design. In Section IV, we

TABLE I
LIST OF MAIN SYMBOLS

W_t	customer load at time slot t
S_t	renewable generation at time slot t
$S_{w,t}$	portion of renewable energy serving load W_t at time slot t
$S_{c,t}$	portion of renewable energy sold to grid at time slot t
$S_{s,t}$	portion of renewable energy stored to battery at time slot t
E_t	energy bought from conventional grid at time slot t
Q_t	portion of E_t stored into battery at time slot t
$F_{d,t}$	amount of energy from battery serving load W_t at time slot t
$F_{s,t}$	amount of energy from battery sold to grid at time slot t
$P_{b,t}$	energy unit buying price from conventional grid at time slot t
$P_{s,t}$	energy unit selling price to conventional grid at time slot t
B_t	battery energy level at time slot t
$x_{e,t}$	entry cost for battery usage at time slot t : $x_{e,t} = 1_{R,t}C_{rc} + 1_{D,t}C_{dc}$
$x_{u,t}$	net change of battery energy level in time slot t : $x_{u,t} = Q_t + S_{r,t} - D_t $
\mathbf{a}_t	control actions at time slot t : $\mathbf{a}_t \triangleq [E_t, Q_t, F_{d,t}, F_{s,t}, S_{c,t}, S_{s,t}]$
$\boldsymbol{\mu}_t$	system inputs at time slot t : $\boldsymbol{\mu}_t \triangleq [W_t, S_t, P_{b,t}, P_{s,t}]$
\bar{x}_e	average entry cost for battery usage over T_o slots
\bar{x}_u	average net change of battery energy level over T_o slots
\bar{J}	average cost of buying energy from the grid over T_o slots
$C(\cdot)$	average usage cost function of the battery
T_o	time period in slots considered for system cost minimization
η_c	battery charging efficiency factor
η_d	battery discharging efficiency factor
R_{\max}	maximum charging amount into the battery
D_{\max}	maximum discharging amount from the battery
Γ	$\max\{\eta_c R_{\max}, D_{\max}/\eta_d\}$
B_{\min}	minimum energy required in battery
B_{\max}	maximum energy allowed in battery
C_{rc}	entry cost for battery usage due to each charging activity
C_{dc}	entry cost for battery usage due to each discharging activity
Δ_a	desired change amount of battery energy level in T_o slots

present our real-time energy control algorithm. In Section V, we analyze the performance of our algorithm. Simulation results are provided in Section VI, and followed by conclusion in Section VII.

Notations: The main symbols used in this paper are summarized in Table I.

II. SYSTEM MODEL

We consider a residential-side energy storage management (ESM) system as shown in Fig. 1. The system contains an energy storage battery which is connected to an on-site renewable generator (RG) and the conventional grid (CG). Energy can be charged into the battery from both the RG and the CG, discharged from the battery for customer electricity demand, or sell back to the CG. Both the RG and the CG can directly supply energy to the customer. We assume the ESM

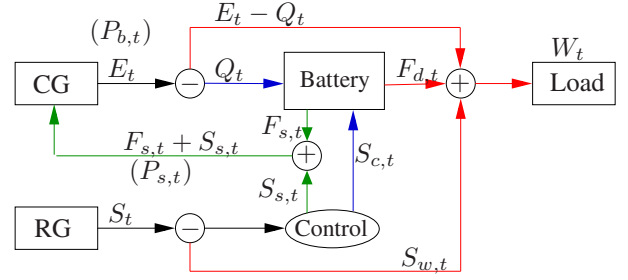


Fig. 1. An ESM system with RG and bidirectional energy flow from/to CG.

system operates in discrete time slots with $t \in \{1, 2, \dots\}$, and all energy control operations are performed per time slot t .

1) *RG:* Let S_t be the amount of energy harvested from the RG at time slot t . Due to the uncertainty of the renewable source, S_t is random. We assume no prior knowledge of S_t or its statistics. Let W_t be the customer load at time slot t . We assume a priority of using S_t to directly serve W_t . Let $S_{w,t}$ be this portion of S_t at time slot t . We have $S_{w,t} = \min\{W_t, S_t\}$. A controller will determine whether the remaining portion, if any, should be stored into the battery and/or sold back to the CG. We denote the stored amount and sold amount by $S_{c,t}$ and $S_{s,t}$, respectively, satisfying

$$S_{c,t} + S_{s,t} \in [0, S_t - S_{w,t}]. \quad (1)$$

2) *CG:* The customer can buy energy from or sell energy to the CG at real-time unit buying price $P_{b,t} \in [P_b^{\min}, P_b^{\max}]$ and selling price $P_{s,t} \in [P_s^{\min}, P_s^{\max}]$, respectively. Both $P_{b,t}$ and $P_{s,t}$ are known at time slot t . To avoid energy arbitrage, the buying price is strictly greater than the selling price at any time, i.e., $P_{b,t} > P_{s,t}$. Let E_t denote the amount of energy bought from the CG at time slot t . Let Q_t denote the portion of E_t that is stored into the battery. The remaining portion $E_t - Q_t$ directly serves the customer load. Let $F_{s,t}$ denote the amount of energy from the battery that is sold back to the CG. The total energy sold from the battery and the RG is bounded by

$$F_{s,t} + S_{s,t} \in [0, U_{\max}] \quad (2)$$

where U_{\max} is the maximum amount of energy that can be sold back to the CG¹.

Note that while $S_{s,t}$ from the RG can be sold back to the CG at any time, energy buying from or selling to the CG should not happen at the same time to avoid energy arbitrage, which is ensured by the constraint $P_{b,t} > P_{s,t}$. With this constraint, we expect the following condition to be satisfied

$$E_t \cdot F_{s,t} = 0. \quad (3)$$

We will verify that our proposed algorithm satisfies (3) in Section V.

3) *Battery Storage:* The battery operation for storage causes the battery to deteriorate, contributing to the storage cost that has been ignored in many prior works. We model battery charging and discharging activities and the degradation cost associate to them as follows.

¹This amount may be regulated by the utility.

i) **Storage operation:** The battery can be charged from multiple sources (*i.e.*, the CG and the RG) at the same time. The total charging amount at time slot t should satisfy

$$S_{c,t} + Q_t \in [0, R_{\max}] \quad (4)$$

where R_{\max} is the maximum charging amount per time slot. Similarly, energy stored in the battery can be used to either serve the customer load and/or sell back to the CG. Let $F_{d,t}$ denote the amount of energy from the battery used to serve the customer at time slot t . The total amount of energy discharged is bounded by

$$F_{d,t} + F_{s,t} \in [0, D_{\max}] \quad (5)$$

where D_{\max} is the maximum discharging amount per time slot. We assume that there is no simultaneous charging and discharging, *i.e.*,

$$(S_{c,t} + Q_t) \cdot (F_{d,t} + F_{s,t}) = 0. \quad (6)$$

Let B_t be the battery energy level at time slot t , bounded by

$$B_t \in [B_{\min}, B_{\max}] \quad (7)$$

where B_{\min} and B_{\max} are the minimum energy required and maximum energy allowed in the battery, respectively, whose values depend on the battery type and capacity. Based on charging and discharging activities and taking the battery charging/discharging inefficiency into account, B_t evolves over time as

$$B_{t+1} = B_t + \eta_c(S_{c,t} + Q_t) - (F_{d,t} + F_{s,t})/\eta_d \quad (8)$$

where η_c and η_d denote the battery charging and discharging efficiency factors, respectively, with $\eta_c, \eta_d \in [0, 1]$.

Finally, the demand-and-supply balance requirement is given by

$$W_t = E_t - Q_t + S_{w,t} + F_{d,t}. \quad (9)$$

ii) **Battery degradation cost:** It is well known that frequent charging/discharging activities cause a battery to degrade [29]. We model two types of battery degradation cost: *entry cost* and *usage cost*. The entry cost is a fixed cost incurred due to each charging or discharging activity. Define two indicator functions to represent charging and discharging activities: $1_{R,t} = \{1 : \text{if } Q_t + S_{c,t} > 0; 0 : \text{otherwise}\}$ and $1_{D,t} = \{1 : \text{if } F_{d,t} + F_{s,t} > 0; 0 : \text{otherwise}\}$. Denote the entry cost for charging by C_{rc} and that for discharging by C_{dc} . The entry cost for battery usage at time slot t is given by $x_{e,t} \triangleq 1_{R,t}C_{rc} + 1_{D,t}C_{dc}$.

The battery usage cost is the cost associated with the charging/discharging amount. Define the net change of battery energy level at time slot t by $x_{u,t} \triangleq |\eta_c(Q_t + S_{c,t}) - (F_{d,t} + F_{s,t})/\eta_d|$. From (4) and (5), it follows that $x_{u,t}$ is bounded by

$$x_{u,t} \in [0, \Gamma] \quad (10)$$

where $\Gamma \triangleq \max\{\eta_c R_{\max}, D_{\max}/\eta_d\}$.² It is known that typically faster charging/discharging, *i.e.*, larger $x_{u,t}$, has a more

detrimental effect on the life time of the battery. Thus, we assume the associated cost function for usage $x_{u,t}$, denoted by $C(\cdot)$, is a continuous, convex, non-decreasing function with maximum derivative $C'(\cdot) < \infty$.

III. PROBLEM FORMULATION

For the ESM system, the system cost includes the energy buying cost minus selling profit and the battery degradation cost. Within a pre-defined T_o -slot time period, the average net cost of energy buying and selling over the CG is given by $\bar{J} \triangleq \frac{1}{T_o} \sum_{t=0}^{T_o-1} E_t P_{b,t} - (F_{s,t} + S_{s,t}) P_{s,t}$. For the battery operation, the average entry cost and average net change over the T_o -slot period are respectively given by

$$\bar{x}_e \triangleq \frac{1}{T_o} \sum_{t=0}^{T_o-1} x_{e,t}, \quad \bar{x}_u \triangleq \frac{1}{T_o} \sum_{t=0}^{T_o-1} x_{u,t} \quad (11)$$

where by (10), \bar{x}_u is bounded by

$$\bar{x}_u \in [0, \Gamma], \quad (12)$$

and the battery average usage cost is $C(\bar{x}_u)$. Thus, the average battery degradation cost over the T_o -slot period is $\bar{x}_e + C(\bar{x}_u)$.

Denote the system inputs by $\boldsymbol{\mu}_t \triangleq [W_t, S_t, P_{b,t}, P_{s,t}]$ and the control actions for energy storage management by $\mathbf{a}_t \triangleq [E_t, Q_t, F_{d,t}, F_{s,t}, S_{c,t}, S_{s,t}]$ at time slot t . With only current input $\boldsymbol{\mu}_t$ known, our objective is to determine a control policy $\{\pi_t\}$ for \mathbf{a}_t (*i.e.*, a mapping $\pi_t : \boldsymbol{\mu}_t \rightarrow \mathbf{a}_t, t = 0, \dots, T_o - 1$) to minimize the average system cost within the T_o -slot period. This is a stochastic control optimization problem and is formulated by

$$\mathbf{P1:} \quad \min_{\{\pi_t\}_{t=0}^{T_o-1}} \bar{J} + \bar{x}_e + C(\bar{x}_u)$$

s.t. (1), (2), (6), (9), (12), and

$$0 \leq S_{c,t} + Q_t \leq \min\{R_{\max}, (B_{\max} - B_t)/\eta_c\} \quad (13)$$

$$0 \leq F_{d,t} + F_{s,t} \leq \min\{D_{\max}, \eta_d(B_t - B_{\min})\} \quad (14)$$

where constraints (13) and (14) are the derived results of constraints (4)–(8).

P1 is a difficult stochastic optimization problem due to the finite time period and the correlated control actions $\{\mathbf{a}_t\}$ over time as a result of time-coupling dynamics of B_t in (8). Furthermore, the input distributions in $\boldsymbol{\mu}_t$ are unknown. The optimal control policy is difficult to obtain. Instead, we develop a real-time algorithm for control action \mathbf{a}_t over time which provides a suboptimal solution for **P1** with the cost objective being reduced as small as possible. In the following, we first summarize our approach and technique to develop this real-time algorithm and then present details.

A. Summary of Our Approach

We develop our real-time algorithm for **P1** using the technique of Lyapunov optimization [25], which is powerful to design dynamic control. However, to use Lyapunov optimization, the problem needs to have time-averaged objective function and constraints, which is not the case for **P1**. To overcome these difficulties, we first modify **P1** and then transfer the modified problem to an equivalent problem **P3**

²Accurate modeling of the battery deterioration due to charging and discharging activities is a challenging problem. Some recent work provides more detailed study on practical modeling of deterioration due to battery operation [30].

that belongs to the class of stochastic optimization problem that Lyapunov optimization technique can be applied to. Then, using Lyapunov technique, we develop our real-time algorithm to determine control action \mathbf{a}_t for **P3**. Our algorithm is to solve a per-slot opportunistic optimization problem **P4** for \mathbf{a}_t at each time slot t , for which the solution is presented in Section IV. Finally, since $\{\mathbf{a}_t\}$ is obtained for **P3**, we design parameters of our algorithm in Section IV-B to ensure that it is also feasible to the original problem **P1**.

B. Problem Modification and Transformation

1) *Modification*: To make **P1** tractable, we first remove the coupling of control actions over time by modifying the constraints (13) and (14) on the per-slot charging and discharging amounts. We set the change of B_t over the T_o -slot period, i.e., $B_{T_o} - B_0$, to be a desired value Δ_a . From (8), this means

$$\frac{1}{T_o} \sum_{\tau=0}^{T_o-1} [\eta_c(Q_\tau + S_{r,\tau}) - (F_{d,\tau} + F_{s,\tau})/\eta_d] = \frac{\Delta_a}{T_o} \quad (15)$$

where by (4)(5)(7), we have $|\Delta_a| \leq \Delta_{\max}$, with $\Delta_{\max} \triangleq \min\{B_{\max} - B_{\min}, T_o \max\{\eta_c R_{\max}, D_{\max}/\eta_d\}\}$. We now modify **P1** to the follow optimization problem

$$\begin{aligned} \mathbf{P2}: \quad & \min_{\{\pi_t\}_{t=0}^{T_o-1}} \bar{J} + \bar{x}_e + C(\bar{x}_u) \\ \text{s.t.} \quad & (1), (2), (4), (5), (6), (9), (12), (15). \end{aligned}$$

From **P1** to **P2**, by imposing the new constraint (15), we remove the dependency of per-slot charging/discharging amount on B_t in constraints (13) and (14), and replace them by (4) and (5), respectively.

We point out that Δ_a in (15) is only a desired value we set in **P2**. For a feasible control algorithm for **P1**, only the constraints in **P1** need to be satisfied. Thus, our designed control algorithm may not satisfy constraint (15) at the end of T_o -slot period.³ This point is further discussed in Section IV-B, and in Section V, we will quantify the amount of mismatch with respect to Δ_a under our proposed control algorithm.

2) *Problem Transformation*: The objective of **P2** contains $C(\bar{x}_u)$ which is a cost function of a time-averaged net change \bar{x}_u . Directly dealing with such function is difficult. Adopting the technique introduced in [31], we transform the problem to one that contains the time-averaged function. To do so, we introduce an auxiliary variable γ_t and its time average $\bar{\gamma} \triangleq \frac{1}{T_o} \sum_{\tau=0}^{T_o-1} \gamma_\tau$ satisfying

$$\gamma_t \in [0, \Gamma], \quad \forall t \quad (16)$$

$$\bar{\gamma} = \bar{x}_u. \quad (17)$$

These constraints ensure that the auxiliary variable γ_t and $x_{u,t}$ lie in the same range and have the same time-averaged behavior. Define $\overline{C(\gamma)} \triangleq \frac{1}{T_o} \sum_{t=0}^{T_o-1} C(\gamma_t)$ as the time average of $C(\gamma_t)$. By using γ_t instead of $x_{u,t}$, we replace constraint (12) with (16) and (17), and transform **P2** into the following problem which is to optimize the control policy $\{\pi_t'\}$ for

³We use **P2** as an intermediate step to design the control algorithm for **P1**. Thus, the proposed algorithm provides an approximate solution for **P2** that may not satisfy (15).

(γ_t, \mathbf{a}_t) (i.e., $\pi_t' : \mu_t \rightarrow (\gamma_t, \mathbf{a}_t)$, $t = 0, \dots, T_o-1$) to minimize the T_o -slot time average of system cost

$$\begin{aligned} \mathbf{P3}: \quad & \min_{\{\pi_t'\}_{t=0}^{T_o-1}} \bar{J} + \bar{x}_e + \overline{C(\gamma)} \\ \text{s.t.} \quad & (1), (2), (4), (5), (6), (9), (15), (16), (17). \end{aligned}$$

It can be shown that **P2** and **P3** are equivalent problems (see Appendix A). The modification and transformation from **P1** to **P3** has enabled us to utilize Lyapunov optimization techniques [25] to design real-time control policy to solve **P3**.

C. Real-Time Control via Lyapunov Optimization

To design a real-time algorithm, in Lyapunov optimization, virtual queue is introduced for each time-averaged constraint, and Lyapunov drift for the queues is defined. It is shown that keeping the stability of each queue is equivalent to satisfying the constraint [25]. Thus, instead of the original cost objective in the optimization problem, a drift-plus-cost metric is considered in Lyapunov optimization and real-time algorithm is developed to minimize this metric. In the following, we develop our algorithm using this technique.

1) *Virtual queues*: Based on the Lyapunov framework, we introduce two virtual queues Z_t and H_t for time-averaged constraints (15) and (17), respectively, as

$$Z_{t+1} = Z_t + \eta_c(Q_t + S_{c,t}) - (F_{d,t} + F_{s,t})/\eta_d - \frac{\Delta_a}{T_o}, \quad (18)$$

$$H_{t+1} = H_t + \gamma_t - x_{u,t}. \quad (19)$$

From (8) and (18), Z_t and B_t have the following relation

$$Z_t = B_t - A_t \quad (20)$$

where $A_t \triangleq A_o + \frac{\Delta_a}{T_o}t$ in which A_o is a constant shift and $\frac{\Delta_a}{T_o}t$ ensures that the left hand side equality in (15) is satisfied. We will revisit the value of A_o to ensure a feasible solution for **P1**.

2) *Lyapunov drift*: Define $\Theta_t \triangleq [Z_t, H_t]$. Define the quadratic Lyapunov function $L(\Theta_t) \triangleq \frac{1}{2}(Z_t^2 + H_t^2)$. Divide T_o slots into M sub-frames of T -slot duration as $T_o = MT$, for $M, T \in \mathbb{N}^+$. We define a one-slot sample path Lyapunov drift as $\Delta(\Theta_t) \triangleq L(\Theta_{t+1}) - L(\Theta_t)$, which only depends on the current system inputs μ_t .

3) *Drift-plus-cost metric*: We define a drift-plus-cost metric which is a weighted sum of the drift $\Delta(\Theta_t)$ and the system cost at current time slot t , given by

$$\Delta(\Theta_t) + V[E_t P_{b,t} - (F_{s,t} + S_{s,t})P_{s,t} + x_{e,t} + C(\gamma_t)] \quad (21)$$

where constant $V > 0$ sets the relative weight between the drift and the system cost. In Lyapunov optimization, instead of minimizing the system cost objective in **P3**, we aim to minimize this drift-to-cost metric. However, directly using this metric to design a control policy is still difficult. Instead, we obtain an upper bound on the drift $\Delta(\Theta_t)$, which will be used for designing our real-time control algorithm.

Lemma 1: Lyapunov drift $\Delta(\Theta_t)$ is upper bounded by

$$\Delta(\Theta_t) \leq Z_t \left(E_t + S_{c,t} + S_{w,t} - W_t - F_{s,t} - \frac{\Delta_a}{T_o} \right)$$

$$+ H_t \gamma_t - g(H_t)(E_t + S_{c,t} + l_t) + G \quad (22)$$

where $G \triangleq \frac{1}{2} \max \left\{ (\eta_c R_{\max} - \frac{\Delta_a}{T_o})^2, (D_{\max}/\eta_d + \frac{\Delta_a}{T_o})^2 \right\} + \frac{1}{2} \Gamma^2$, and

$$g(H_t) \triangleq \begin{cases} \eta_c H_t & H_t \geq 0 \\ H_t/\eta_d & H_t < 0 \end{cases} \quad (23)$$

$$l_t \triangleq \text{sgn}(H_t)(S_{w,t} - W_t - F_{s,t}) \quad (24)$$

where $\text{sgn}(\cdot)$ is the sign function.

Proof: See Appendix B. ■

By Lemma 1, an upper bound on the per-slot drift-plus-cost metric in (21) is readily obtained. In the following, we use this upper bound to develop a real-time control algorithm.

IV. REAL-TIME BIDIRECTIONAL CONTROL ALGORITHM

We now propose our real-time control algorithm to minimize the upper bound on the drift-plus-cost metric *per slot*. Removing all the constant terms in the upper bound of the drift-plus-cost metric that are independent of \mathbf{a}_t and γ_t , we have the equivalent optimization problem which can be further separated into two sub problems for γ_t and \mathbf{a}_t , respectively, as follows

$$\mathbf{P4}_a : \min_{\gamma_t} H_t \gamma_t + VC(\gamma_t) \quad \text{s.t.} \quad (16).$$

$$\mathbf{P4}_b : \min_{\mathbf{a}_t} E_t(Z_t - g(H_t) + VP_{b,t}) + S_{c,t}(Z_t - g(H_t)) - F_{s,t}(Z_t - |g(H_t)| + VP_{s,t}) - S_{s,t}VP_{s,t} + Vx_{e,t} \quad \text{s.t.} \quad (1), (2), (4), (5), (6), (9), (15).$$

First, we solve $\mathbf{P4}_a$ to obtain the optimal solution γ_t^* . Note that $\mathbf{P4}_a$ is convex for $C(\cdot)$ being convex. Thus, we can directly solve it and obtain the optimal γ_t^* of $\mathbf{P4}_a$.

Lemma 2: The optimal solution γ_t^* of $\mathbf{P4}_a$ is given by

$$\gamma_t^* = \begin{cases} 0 & \text{if } H_t \geq 0 \\ \Gamma & \text{if } H_t < -VC'(\Gamma) \\ C'^{-1}(-\frac{H_t}{V}) & \text{otherwise} \end{cases} \quad (25)$$

where $C'(\cdot)$ is the first derivative of $C(\cdot)$, and $C'^{-1}(\cdot)$ the inverse function of $C'(\cdot)$.

Proof: See Appendix C. ■

Next, we obtain the optimal \mathbf{a}_t^* of $\mathbf{P4}_b$ and provide the conditions under which \mathbf{a}_t^* is feasible to $\mathbf{P1}$.

A. The Optimal Control \mathbf{a}_t^* for $\mathbf{P4}_b$

Denote the objective function of $\mathbf{P4}_b$ by $J(\mathbf{a}_t)$. Define the *idle state* of the battery as the state where there is no charging or discharging activity. The control decision in the idle state is given by $\mathbf{a}_t^{\text{id}} = [E_t^{\text{id}}, Q_t^{\text{id}}, F_{d,t}^{\text{id}}, F_{s,t}^{\text{id}}, S_{c,t}^{\text{id}}, S_{s,t}^{\text{id}}]$, where $E_t^{\text{id}} = W_t - S_{w,t}$, $Q_t^{\text{id}} = F_{d,t}^{\text{id}} = F_{s,t}^{\text{id}} = S_{c,t}^{\text{id}} = 0$, and $S_{s,t}^{\text{id}} = \min\{S_t - S_{w,t}, U_{\max}\}$. Then, in the idle state, we have $J(\mathbf{a}_t^{\text{id}}) = (W_t - S_{w,t})(Z_t - g(H_t) + VP_{b,t}) - VP_{s,t} \min\{S_t - S_{w,t}, U_{\max}\}$. We derive the optimal control decision $\mathbf{a}_t^* = [E_t^*, Q_t^*, F_{d,t}^*, F_{s,t}^*, S_{c,t}^*, S_{s,t}^*]$ in five cases in Proposition 1 below. Define $[a]^+ \triangleq \max\{a, 0\}$.

Proposition 1: Define $(S_{c,t}^a, S_{s,t}^a)$ as follows: If $VP_{s,t} \geq g(H_t) - Z_t$: $S_{s,t}^a \triangleq \min\{S_t - S_{w,t}, U_{\max}\}$, $S_{c,t}^a \triangleq \min\{S_t -$

$S_{w,t} - S_{s,t}^a, R_{\max}\}$; Otherwise, $S_{c,t}^a \triangleq \min\{S_t - S_{w,t}, R_{\max}\}$, $S_{s,t}^a \triangleq \min\{S_t - S_{w,t} - S_{c,t}^a, U_{\max}\}$.

Denote $\mathbf{a}_t^w = [E_t^w, Q_t^w, F_{d,t}^w, F_{s,t}^w, S_{c,t}^w, S_{s,t}^w]$ as the control decision in the charging or discharging state. The optimal control solution \mathbf{a}_t^* for $\mathbf{P4}_b$ is given in the following cases:

1) For $Z_t - g(H_t) + VP_{b,t} \leq 0$: The battery is in either the charging state or the idle state. Let

$$\begin{cases} F_{d,t}^w = F_{s,t}^w = 0, & S_{c,t}^w = S_{c,t}^a, & S_{s,t}^w = S_{s,t}^a \\ Q_t^w = R_{\max} - S_{c,t}^w \\ E_t^w = W_t - S_{w,t} + R_{\max} - S_{c,t}^w. \end{cases} \quad (26)$$

Then, $\mathbf{a}_t^* = \arg \min_{\mathbf{a}_t \in \{\mathbf{a}_t^w, \mathbf{a}_t^{\text{id}}\}} J(\mathbf{a}_t)$.

2) For $\max\{Z_t - g(H_t), Z_t - |g(H_t)| + VP_{s,t}\} < 0 \leq Z_t - g(H_t) + VP_{b,t}$: The battery is in either the charging state (from the RG only), the discharging state (to the customer load only), or the idle state. Let

$$\begin{cases} F_{d,t}^w = \min\{W_t - S_{w,t}, D_{\max}\} \\ F_{s,t}^w = Q_t^w = 0, & S_{c,t}^w = S_{c,t}^a, & S_{s,t}^w = S_{s,t}^a \\ E_t^w = [W_t - S_{w,t} - D_{\max}]^+. \end{cases} \quad (27)$$

Then, $\mathbf{a}_t^* = \arg \min_{\mathbf{a}_t \in \{\mathbf{a}_t^w, \mathbf{a}_t^{\text{id}}\}} J(\mathbf{a}_t)$.

3) For $Z_t - g(H_t) \leq 0 \leq Z_t - |g(H_t)| + VP_{s,t}$: The battery is in either the charging state (from the RG only), the discharging state, or the idle state. Define \mathbf{a}_t^{dc} in the discharging state as

$$\begin{cases} F_{d,t}^{\text{dc}} = \min\{W_t - S_{w,t}, D_{\max}\} \\ S_{s,t}^{\text{dc}} = \min\{S_t - S_{w,t}, U_{\max}\} \\ F_{s,t}^{\text{dc}} = \min\{D_{\max} - F_{d,t}^{\text{dc}}, U_{\max} - S_{s,t}^{\text{dc}}\} \\ S_{c,t}^{\text{dc}} = Q_t^{\text{dc}} = 0, & E_t^{\text{dc}} = [W_t - S_{w,t} - D_{\max}]^+; \end{cases} \quad (28)$$

Define \mathbf{a}_t^{rc} in the charging state as

$$\begin{cases} F_{d,t}^{\text{rc}} = F_{s,t}^{\text{rc}} = Q_t^{\text{rc}} = 0 \\ S_{c,t}^{\text{rc}} = S_{c,t}^a, & S_{s,t}^{\text{rc}} = S_{s,t}^a \\ E_t^{\text{rc}} = W_t - S_{w,t}. \end{cases} \quad (29)$$

Then, $\mathbf{a}_t^* = \arg \min_{\mathbf{a}_t \in \{\mathbf{a}_t^{\text{rc}}, \mathbf{a}_t^{\text{dc}}, \mathbf{a}_t^{\text{id}}\}} J(\mathbf{a}_t)$.

4) For $Z_t - |g(H_t)| + VP_{s,t} < 0 \leq Z_t - g(H_t)$: The battery is in either the discharging state (to the customer load only) or the idle state. Let

$$\begin{cases} F_{d,t}^w = \min\{W_t - S_{w,t}, D_{\max}\} \\ F_{s,t}^w = Q_t^w = 0 \\ S_{s,t}^w = \min\{S_t - S_{w,t}, U_{\max}\}, & S_{c,t}^w = 0 \\ E_t^w = [W_t - S_{w,t} - D_{\max}]^+. \end{cases} \quad (30)$$

Then, $\mathbf{a}_t^* = \arg \min_{\mathbf{a}_t \in \{\mathbf{a}_t^w, \mathbf{a}_t^{\text{id}}\}} J(\mathbf{a}_t)$.

5) For $\min\{Z_t - g(H_t), Z_t - |g(H_t)| + VP_{s,t}\} > 0$: The battery is in either the discharging state or the idle state. If $Z_t > |g(H_t)|$, let

$$\begin{cases} F_{d,t}^w = \min\{W_t - S_{w,t}, D_{\max}\} \\ F_{s,t}^w = \min\{D_{\max} - F_{d,t}^w, U_{\max}\} \\ S_{s,t}^w = \min\{S_t - S_{w,t}, U_{\max} - F_{s,t}^w\} \\ S_{c,t}^w = Q_t^w = 0, & E_t^w = [W_t - S_{w,t} - D_{\max}]^+; \end{cases} \quad (31)$$

Otherwise, let

$$\begin{cases} F_{d,t}^w = \min\{W_t - S_{w,t}, D_{\max}\} \\ S_{s,t}^w = \min\{S_t - S_{w,t}, U_{\max}\} \\ F_{s,t}^w = \min\{D_{\max} - F_{d,t}^w, U_{\max} - S_{s,t}^w\} \\ S_{c,t}^w = Q_t^w = 0, E_t^w = [W_t - S_{w,t} - D_{\max}]^+. \end{cases} \quad (32)$$

Then, $\mathbf{a}_t^* = \arg \min_{\mathbf{a}_t \in \{\mathbf{a}_t^w, \mathbf{a}_t^{\text{id}}\}} J(\mathbf{a}_t)$.

Proof: See Appendix D. \blacksquare

Proposition 1 provides the closed-form control solution in five cases, depending on the battery energy level (via Z_t), battery usage cost (via H_t), and the prices. In each case, $J(\mathbf{a}_t^w)$ in the charging (or discharging) state is compared with $J(\mathbf{a}_t^{\text{id}})$ in the idle state, and the optimal \mathbf{a}_t^* is the control solution of the state with the minimum objective value.

Remarks: Note that there are two sources to be controlled for selling energy back: $F_{s,t}$ from the battery and $S_{s,t}$ from the RG. From Proposition 1, whether or not to sell energy from the battery back to the grid depends on the battery energy level. When the battery energy level is low (Case 1), energy is kept in the battery. When the battery has a moderately low energy level (Case 2), it may be in either the charging or discharging state. For the latter, the battery only supplies enough energy to the customer but does not sell energy back. When the battery energy level is higher but still moderate (Case 3), it may still be in either the charging or discharging state. For the latter, the battery may sell energy back to the grid. When the battery has just sufficient energy (Case 4), it may supply energy to the customer, but will not sell energy back to the grid. When the energy level in the battery is high (Cases 5), it may supply energy to the customer and at the same time sell energy back. In contrast, the renewable energy can be sold to the grid regardless of the battery energy level, state (charging, discharging, or idle), or the price to make an additional profit. As the result, energy generated by the renewable will be utilized as much as possible. However, when the system wants to sell energy from both the battery and the renewable, the order to determine $S_{s,t}$ and $F_{s,t}$ depends on which results in the minimum cost in $\mathbf{P4}_b$. In Case 5, for the control decision in (31), $S_{s,t}$ is determined after $F_{s,t}$, while in (32), $F_{s,t}$ is determined after $S_{s,t}$.

B. Feasible $\{\mathbf{a}_t^*\}$ for $\mathbf{P1}$

The optimal solution \mathbf{a}_t^* of $\mathbf{P4}_b$ provides a real-time solution for $\mathbf{P3}$. However, it may not be feasible to $\mathbf{P1}$, because the battery capacity constraint (7) on B_t may be violated. By properly designing A_o and V , we can guarantee that \mathbf{a}_t^* satisfies constraint (7), and ensure the feasibility of the solution. Define $[a]_- \triangleq \min\{a, 0\}$. The result is stated below.

Proposition 2: For the proposed real-time control algorithm, by setting $V \in (0, V_{\max}]$ with

$$V_{\max} = \frac{B_{\max} - B_{\min} - \eta_c R_{\max} - (D_{\max} + 2\Gamma)/\eta_d - |\Delta_a|}{P_b^{\max} + C'(\Gamma)/\eta_d + [C'(\Gamma)/\eta_d - P_s^{\min}]^+}, \quad (33)$$

Algorithm 1 Real-time battery management control algorithm

Initialize: $Z_0 = H_0 = 0$.

Determine T_o .

Set $\Delta_a \in [-\Delta_{\max}, \Delta_{\max}]$.

Set A_o and $V \in (0, V_{\max}]$ as in (34) and (33), respectively.

At time slot t :

- 1: Observe the system inputs $\boldsymbol{\mu}_t$ and queues Z_t and H_t .
- 2: Solve $\mathbf{P4}_a$ and obtain γ_t^* in (25); Solve $\mathbf{P4}_b$ and obtain \mathbf{a}_t^* by following cases (26)-(32) in Proposition 1.
- 3: Use \mathbf{a}_t^* and γ_t^* to update Z_{t+1} and H_{t+1} in (18) and (19), respectively.
- 4: Output control decision \mathbf{a}_t^* .

and A_t in (20) with

$$A_o = B_{\min} + V P_b^{\max} + \frac{VC'(\Gamma) + \Gamma + D_{\max}}{\eta_d} + \frac{\Delta_a}{T_o} - [\Delta_a]_-, \quad (34)$$

B_t satisfies the battery capacity constraint (7), and control solution \mathbf{a}_t^* of $\mathbf{P4}_b$, for any t , is feasible to $\mathbf{P1}$.

Proof: See Appendix E. \blacksquare

Note that $V_{\max} > 0$ in (33) is generally satisfied for practical battery storage capacity and $|\Delta_a|$ being set relatively small. We should also point out that since Δ_a is a desired value set by our proposed algorithm, the solution \mathbf{a}_t^* of $\mathbf{P4}_b$ may not necessarily satisfy constraint (15) at the end of the T_o -slot period, and thus may not be feasible to $\mathbf{P2}$. However, Proposition 2 provides the values of A_o and V to guarantee the control solutions $\{\mathbf{a}_t^*\}$ being feasible to $\mathbf{P1}$.

The proposed real-time bidirectional energy control algorithm is summarized in Algorithm 1. We emphasize that i) our proposed algorithm does not require or rely on any statistical distributions of system inputs $\boldsymbol{\mu}_t$ (prices, load, and renewable generation processes), and thus can be applied to general scenarios, especially when these processes are non-ergodic or difficult to predict in a highly dynamic environment. ii) The control solution provided by our real-time algorithm is given in closed-form which requires little computation, and thus is attractive for practical implementation.

V. PERFORMANCE ANALYSIS

To analyze the performance of our real-time solution in Algorithm 1 with respect to $\mathbf{P1}$, let $u^*(V)$ denote the T_o -slot average system cost objective of $\mathbf{P1}$ achieved by Algorithm 1, which depends on the value of V set by Algorithm 1. For comparison, we partition T_o slots into T frames with $T_o = MT$, for some integers $M, T \in \mathbb{N}^+$. Within each frame m , we consider a T -slot look-ahead optimal control policy, where $\{W_t, S_t, P_{b,t}, P_{s,t}\}$ are known non-causally for the entire frame beforehand. Let u_m^{opt} denote the minimum T -slot average cost for frame m achieved by this optimal policy. We can view u_m^{opt} as the minimum objective value of $\mathbf{P1}$ with $T_o = T$ under the optimal T -slot look-ahead solution. The performance gap of our proposed real-time algorithm to the optimal T -slot look-ahead policy is bounded in the following theorem.

Theorem 1: For any arbitrary system inputs $\{\mu_t\}$, and any $M, T \in \mathbb{N}^+$ with $T_o = MT$, the T_o -slot average system cost under Algorithm 1 to that under the optimal T -slot look-ahead policy satisfies

$$\begin{aligned} u^*(V) - \frac{1}{M} \sum_{m=0}^{M-1} u_m^{\text{opt}} \\ \leq \frac{GT}{V} + \frac{L(\Theta_0) - L(\Theta_{T_o})}{VT_o} + \frac{C'(\Gamma)(H_0 - H_{T_o})}{T_o} \end{aligned} \quad (35)$$

with the bound at the right hand side being finite. Asymptotically as $T_o \rightarrow \infty$,

$$\lim_{T_o \rightarrow \infty} u^*(V) - \lim_{T_o \rightarrow \infty} \frac{1}{M} \sum_{m=0}^{M-1} u_m^{\text{opt}} \leq \frac{GT}{V}. \quad (36)$$

Proof: See Appendix F. ■

By Theorem 1, the performance gap of Algorithm 1 to the T -slot look-ahead optimal policy is upper bounded in (35), for any T with $T_o = MT$. To minimize the gap, we should always set $V = V_{\max}$. From (36), as the duration goes to infinity, the asymptotic gap is in the order of $\mathcal{O}(1/V)$. Since V_{\max} increases with B_{\max} , When $V = V_{\max}$, Algorithm 1 is asymptotically equivalent to the T -slot look-ahead optimal policy as the battery capacity and time duration increases.

As discussed at the end of Section IV-B, constraint (15) in **P2** sets a desired value for Δ_a which may not be achieved by our proposed algorithm at the end of T_o slots. Denote this mismatch under Algorithm 1 by $\epsilon \triangleq \sum_{\tau=0}^{T_o-1} (Q_\tau + S_{r,\tau} - F_{s,\tau} - F_{d,\tau}) - \Delta_a$. This mismatch is quantified below.

Proposition 3: For any arbitrary system inputs $\{\mu_t\}$ and any initial queue value $Z_0 \in \mathbb{R}$, the mismatch for constraint (15) by Algorithm 1 is given by $\epsilon = Z_{T_o} - Z_0$, and is bounded by

$$\begin{aligned} |\epsilon| \leq 2\Gamma/\eta_d + VC'(\Gamma)/\eta_d + V[C'(\Gamma)/\eta_d - P_s^{\min}]^+ \\ + VP_b^{\max} + \eta_c R_{\max} + D_{\max}/\eta_d. \end{aligned} \quad (37)$$

Proof: See Appendix G. ■

Finally, we expect constraint (3) to be satisfied by Algorithm 1, *i.e.*, buying energy ($E_t > 0$) and selling stored energy ($F_{s,t} > 0$) should not occur at same time. This is verified in the following result.

Proposition 4: For any system inputs μ_t , the optimal control solution \mathbf{a}_t^* under Algorithm 1 guarantees constraint (3) being satisfied.

Proof: See Appendix H. ■

VI. SIMULATION RESULTS

We set the slot duration to be 5 minutes, and assume that system input μ_t remains unchanged within each slot. We set the buying price $P_{b,t}$ using the data collected from Ontario Energy Board [32]. We use solar energy for the RG to generate $\{S_t\}$. As a result, $\{S_t\}$ is a non-ergodic process, with the mean $\bar{S}_t = \mathbb{E}[S_t]$ changing periodically over 24 hours. As shown in Fig. 2 top, we model $\{\bar{S}_t\}$ by a three-stage pattern as $\{\bar{S}^h, \bar{S}^m, \bar{S}^l\} = \{1.98, 0.96, 0.005\}/12$ kWh, and set standard deviation $\sigma_{S^i} = 0.4\bar{S}^i$, for $i = h, m, l$. We also model the load W_t as a non-ergodic process with mean $\bar{W}_t = \mathbb{E}[W_t]$ following a three-stage pattern over each day as $\{\bar{W}^h, \bar{W}^m, \bar{W}^l\} =$

$\{2.4, 1.38, 0.6\}/12$ kWh, shown in Fig. 2 middle, and set standard deviation $\sigma_{W^i} = 0.2\bar{W}^i$, for $i = h, m, l$. Buying price $P_{b,t}$ follows a three-stage price pattern repeated each day as $\{P_b^h, P_b^m, P_b^l\} = \{\$0.118, \$0.099, \$0.063\}$ per kWh, as shown in Fig. 2 bottom. The battery and storage parameters are set as follows: $B_{\min} = 0$, $R_{\max} = 0.15$ kWh, $D_{\max} = 0.15$ kWh, $C_{rc} = C_{dc} = 0.001$, $U_{\max} = 0.2$ kWh, and the initial battery energy level $B_0 = B_{\max}/2$. Unless specified, we set the following default values: $B_{\max} = 3$ kWh, and $\eta_c = \eta_d = 0.98$.⁴

Quadratic battery usage cost: We use a quadratic function for the battery usage cost as an exemplary case, given by $C(\bar{x}_u) = k\bar{x}_u^2$, where $k > 0$ is the battery cost coefficient depending on the battery specification and \bar{x}_u is given in (11). The optimal γ_t^* of **P4_a** in (25) in this case can be derived as: i) $\gamma_t^* = 0$ for $H_t > 0$; ii) $\gamma_t^* = \Gamma$ for $H_t < -kVT$; iii) $\gamma_t^* = -H_t/(2kV)$ for $-2kVT \leq H_t \leq 0$. We use this cost function throughout our simulation study. Unless specified, we set $k = 0.1$ as the default value.

We consider a 24-hour duration with $T_o = 288$ slots. Since a positive (negative) Δ_a allows battery to charge (discharge) more than discharge (charge) over a T_o -period, we alternate the sign of Δ_a over multiple T_o -slot periods to control this tendency: we set $\Delta_a = +c$ ($-c$) for the odd (even) T_o -slot periods, for some constant $c > 0$. Unless specified, we set $V = V_{\max}$ as the default value.

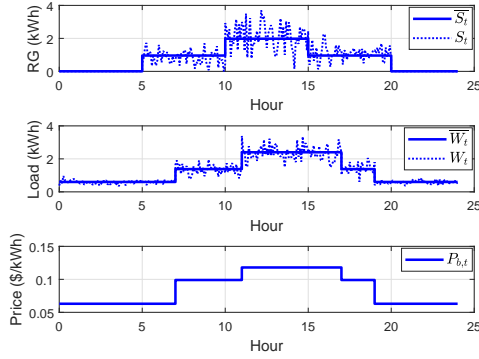
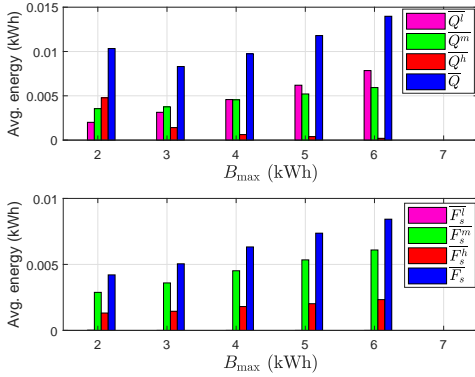
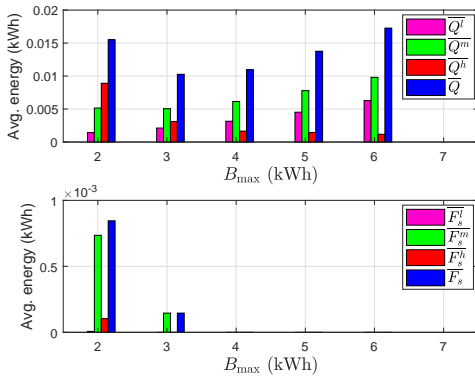
1) *Energy buying and selling vs. prices:* We study the energy buying and selling behaviors under different selling-to-buying price ratios. Define the selling-to-buying price ratio by $\rho_p \triangleq P_{s,t}/P_{b,t}$ with $0 \leq \rho_p < 1$. It is fixed over T_o time slots. Define the average amount of bought and sold energy at each price stage of $P_{b,t}$ (high, medium, low) as

$$\bar{Q}^i \triangleq \frac{1}{|\mathcal{T}_b^i|} \sum_{t \in \mathcal{T}_b^i} Q_t^*, \quad \bar{F}_s^i \triangleq \frac{1}{|\mathcal{T}_s^i|} \sum_{t \in \mathcal{T}_s^i} F_{s,t}^*, \quad i = h, m, l$$

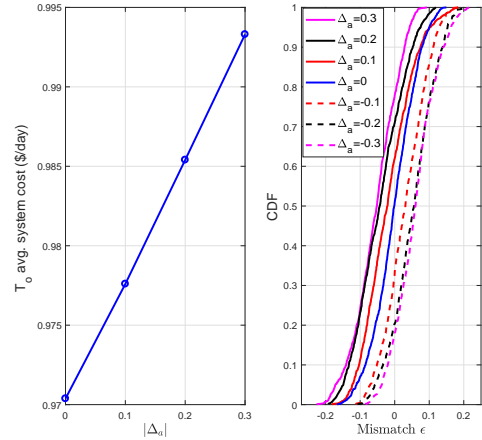
where $\mathcal{T}_b^i \triangleq \{t : P_{b,t} = P_b^i\}$ and $\mathcal{T}_s^i \triangleq \{t : P_{s,t} = P_s^i\}$. Also, denote \bar{Q} and \bar{F}_s as the overall energy bought and sold, respectively. Figs. 3 and 4 show the average amount of energy for $\rho_p = 0.9$ and 0.3 (high and low selling prices), respectively. Comparing Fig. 3 bottom with Fig. 4 bottom, we see that more energy is sold at higher ρ_p to increase the profit, while at lower ρ_p , selling at the price is not cost-effective, and the system tends to keep the energy in the storage for future usage. Furthermore, in Fig. 3 bottom, at higher ρ_p , the average amount of energy sold at P_s^m and P_s^h increases with the battery capacity B_{\max} . This is because a larger capacity offers more flexibility for charging and discharging activities, and allows more energy to be sold back at higher prices. For the same reason, a larger capacity allows more energy to be bought at lower price, as shown in Figs. 3 and 4 top, where, as B_{\max} increases, the amount of energy bought from the grid at higher price $P_{b,t} = P_b^h$ decreases and at lower price $P_{b,t} = P_b^l$ increases.

2) *Setting Δ_a and mismatch ϵ :* Fig. 5 shows how the average system cost varies with Δ_a set by proposed Algorithm 1,

⁴A typical Lithium-ion battery can achieve 0.99 charging efficiency.


 Fig. 2. Example of W_t , S_t and $P_{b,t}$ over 24 hours.

 Fig. 3. Average energy bought (sold) into (from) the battery at different prices (selling-to-buying price ratio $\rho_p = 0.9$).

 Fig. 4. Average energy bought (sold) into (from) the battery at different prices (selling-to-buying price ratio $\rho_p = 0.3$).

for $\rho_p = 0.9$. We simulate the system over multiple T_o -slot periods for a given $|\Delta_a|$. It shows that the system cost increases with $|\Delta_a|$. More energy needs to be bought to be stored in the battery for $\Delta_a > 0$, leading to a higher system cost, while it is the opposite for $\Delta_a < 0$. Overall, the system cost is the smallest when $\Delta_a = 0$. Fig. 5 right shows the CDF of the mismatch ϵ at different value of Δ_a by Algorithm 1. We see that ϵ at different values of Δ_a is relatively small for $\rho_p = 0.9$, as the availability to sell energy helps keep the mismatch relatively small. Also from the sign of ϵ , it shows that the net energy change in the battery over the period tends to be less than $|\Delta_a|$. The mismatch ϵ is the smallest when $\Delta_a = 0$. Based on the above results, we conclude that setting


 Fig. 5. Performance of Algorithm 1 at different Δ_a setting (selling-to-buying price ratio $\rho_p = 0.9$). Left: average system cost at different $|\Delta_a|$; Right: CDF of mismatch ϵ at different Δ_a .

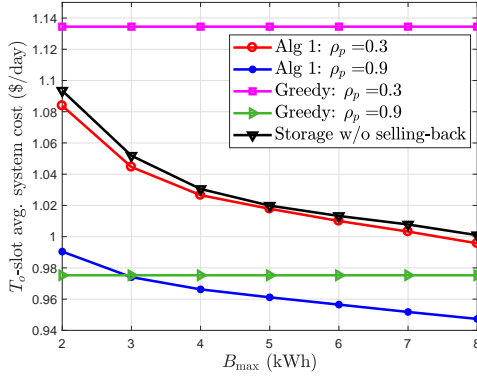
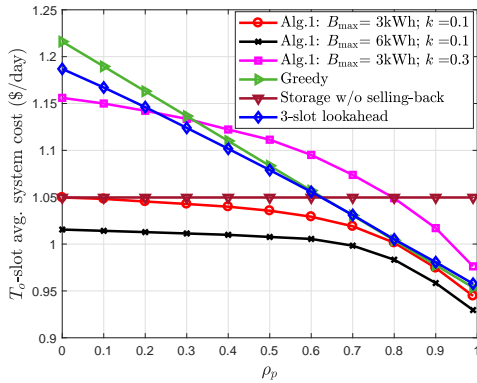
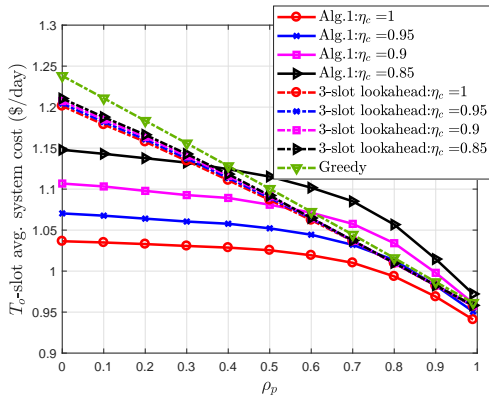
$\Delta_a = 0$ in Algorithm 1 is the most desirable, and is used as the default value for our simulation study.

3) *Performance Comparison*: We consider three other algorithms for comparison: i) *3-slot look-ahead*: The non-causal T -slot look-ahead optimal solution with $T = 3$, where system inputs $\{\mu_t\}$ for each 3-slot frame are known non-causally ahead of time. The resulting 3-slot minimum system cost is u_m^{opt} for frame m .⁵ ii) *Greedy*: A greedy algorithm that minimizes the per-slot system cost, based on the current inputs μ_t . For one-slot cost minimization, to avoid the battery operation cost, the system directly buys energy from the grid to serve the load without storing energy into the battery. Thus, this greedy method is essentially a method without storage. iii) *Storage without selling-back*: With no energy selling-back capability in the model, the problem is reduced to the one considered in [12] and the algorithm proposed therein. Note that among the three methods, the first one is a non-causal approach and the rest are real-time approaches.

Fig. 6 compares the average system cost of different algorithms at different battery capacity B_{max} , where the cost is converted into dollars per day. The system cost under Algorithm 1 reduces as B_{max} increases, because a larger battery capacity gives more flexibility on charging/discharging, allowing the system to buy more energy at a lower price and sell more at a higher price. Also, higher selling-to-buying price ratio $\rho_p = 0.9$ results in a lower average system cost. For the greedy algorithm, since it is essentially a method without the use of storage, the system cost does not vary with the battery capacity. Compared with the greedy algorithm, our proposed Algorithm 1 offers more cost reduction as the battery capacity becomes larger. Moreover, compared with the storage without selling-back, the extra cost saving by the availability to sell back energy at different selling price is clearly seen.

Fig. 7 provides the comparison of system cost at various

⁵The 3-slot look-ahead policy is obtained through exhaustive search. In general, the optimal solution can only be obtained from exhaustive search, which is difficult for larger T .

Fig. 6. Average system cost vs. battery capacity B_{\max} .Fig. 7. Average system cost vs. selling-to-buying price ratio ρ_p (Default: $B_{\max} = 3$ kWh, $k = 0.1$).Fig. 8. Comparison of average system cost over ρ_p at different battery charging (discharging) efficiency $\eta_c (= \eta_d)$.

selling-to-buying price ratio ρ_p values. For other algorithms, default $B_{\max} = 3$ kWh and $k = 0.1$ are used. At the default setting, our proposed algorithm outperforms all other three methods for $\rho_p \in [0, 1]$. By comparing Algorithm 1 with the storage without selling-back method, we see the cost saving by selling extra energy back to the grid at different ρ_p . We also plot the performance of Algorithm 1 at a larger battery capacity and at a higher value of k (higher battery usage cost) to see the effect of different battery specifications on the cost performance.

Finally, in Fig. 8, we show the effect of different battery

charging and discharging efficiencies on the performance, where we set $\eta_c = \eta_d$. Depending on the quality of battery, the efficiency may range from 0.85 to 0.99. As we see, compared to the 3-slot look-ahead solution, the increase of system cost at lower $\eta_c(\eta_d)$ under Algorithm 1 is more noticeable. The performance of the greedy algorithm does not change with different η_c since the algorithm does not use the storage. When the charging efficiency is low (0.85 ~ 0.9) and selling-to-buying price ratio is high, the greedy and 3-slot look-ahead methods can have a lower system cost, indicating that the benefit of storage diminishes in this scenario.

VII. CONCLUSION

In this work, we proposed a real-time bidirectional energy control algorithm for a residential ESM system to minimize the system cost within a given time period. The ESM system has an integrated RG besides connected to the CG, and is capable of buy/sell energy from/to the CG. For the system cost, besides the energy buying cost and selling profit, we included the storage cost by accounting the battery operational cost and inefficiency due to charging/discharging activities. Our real-time algorithm provides a closed-form control solution for the ESM system which is very simple to implement. It does not rely on any statistical knowledge of system inputs and is applicable to arbitrary system input dynamics. We showed that our proposed algorithm provides a bounded performance guarantee to the non-causal T -slot look-ahead optimal control solution. Simulation demonstrated that our proposed algorithm outperforms other non-causal or real-time alternative methods. We further provided simulation study to understand how the availability of selling energy, selling and buying price setting, and battery inefficiency affect the storage behavior and system cost.

APPENDIX A EQUIVALENCE OF PROBLEMS **P2** AND **P3**

The proof follows the general argument in [31]. The optimal solution of **P2** satisfies all constraints of **P3**, and therefore it is a feasible solution of **P3**. Let u_2^o and u_3^o denote the minimum objective values of **P2** and **P3**, respectively. We have $u_3^o \leq u_2^o$. By Jensen's inequality and convexity of $C(\cdot)$, we have $C(\bar{\gamma}) \geq C(\bar{\gamma}) = C(\bar{x}_u)$, which means $u_3^o \geq u_2^o$. Hence, $u_2^o = u_3^o$, and **P2** and **P3** are equivalent.

APPENDIX B PROOF OF LEMMA 1

Proof: By the definition of Lyapunov drift $\Delta(\Theta_t)$,

$$\begin{aligned} \Delta(\Theta_t) &\triangleq L(\Theta_{t+1}) - L(\Theta_t) = \frac{1}{2} (Z_{t+1}^2 - Z_t^2 + H_{t+1}^2 - H_t^2) \\ &= Z_t \left(\eta_c(Q_t + S_{c,t}) - \frac{F_{d,t} + F_{s,t}}{\eta_d} - \frac{\Delta_a}{T_o} \right) \\ &\quad + H_t(\gamma_t - x_{u,t}) + \frac{1}{2}(\gamma_t - x_{u,t})^2 \\ &\quad + \frac{1}{2} \left(\eta_c(Q_t + S_{c,t}) - \frac{F_{d,t} + F_{s,t}}{\eta_d} - \frac{\Delta_a}{T_o} \right)^2. \end{aligned} \quad (38)$$

Let g_t denote the sum of the last two terms in (38). From (15), we have $\frac{\Delta_a}{T_o} \leq \max\{\eta_c R_{\max}, D_{\max}/\eta_d\} = \Gamma$. For a given value of Δ_a , by (4), (5), (10) and (16), g_t is upper bounded by

$$g_t \leq \frac{\max\left\{\left(\eta_c R_{\max} - \frac{\Delta_a}{T_o}\right)^2, \left(\frac{D_{\max}}{\eta_d} + \frac{\Delta_a}{T_o}\right)^2\right\}}{2} + \frac{\Gamma^2}{2} \triangleq G. \quad (39)$$

We now find the upper bound of $-H_t x_{u,t}$ in the second term of (38).

Note that $S_{w,t}$, W_t and H_t are known for the current time slot t . Also note that, $S_{w,t} - W_t \leq 0$, because $S_{w,t} = \min\{W_t, S_t\}$. The upper bound of $-H_t x_{u,t}$ is obtained as follows:

1) For $H_t \geq 0$: Let $l_t \triangleq S_{w,t} - W_t - F_{s,t} \leq 0$. we have $x_{u,t} = |\eta_c(S_{c,t} + Q_t) - (F_{d,t} + F_{s,t})/\eta_d| \geq \eta_c|(S_{c,t} + Q_t) - (F_{d,t} - F_{s,t})| = \eta_c|E_t + S_{c,t} + S_{w,t} - W_t - F_{s,t}|$, where the last equality is by the supply-demand balance requirement in (9). Thus,

$$\begin{aligned} -H_t x_{u,t} &\leq -H_t \eta_c |E_t + S_{c,t} + S_{w,t} - W_t - F_{s,t}| \\ &\leq -H_t \eta_c (|E_t + S_{c,t}| + |S_{w,t} - W_t - F_{s,t}|) \\ &\leq -H_t \eta_c (E_t + S_{c,t} + l_t). \end{aligned}$$

2) For $H_t < 0$: Let $l_t \triangleq W_t - S_{w,t} + F_{s,t} \geq 0$. We have $x_{u,t} \leq |(S_{c,t} + Q_t) - (F_{d,t} + F_{s,t})/\eta_d| = |E_t + S_{c,t} + S_{w,t} - W_t - F_{s,t}|/\eta_d$. Thus,

$$\begin{aligned} -H_t x_{u,t} &\leq -H_t |E_t - F_{s,t} + S_{c,t} + S_{w,t} - W_t|/\eta_d \\ &\leq -H_t (|E_t + S_{c,t}| + |S_{w,t} - W_t| + |F_{s,t}|)/\eta_d \\ &= -H_t/\eta_d (E_t + S_{c,t} + l_t). \end{aligned}$$

Finally, for the first term in (38), we have $Z_t(\eta_c(Q_t + S_{c,t}) - (F_{d,t} + F_{s,t})/\eta_d - \frac{\Delta_a}{T_o}) \leq Z_t(Q_t + S_{c,t} - F_{d,t} - F_{s,t} - \frac{\Delta_a}{T_o}) = Z_t(E_t + S_{c,t} + S_{w,t} - W_t - F_{s,t} - \frac{\Delta_a}{T_o})$. Combining the above results and (39), we have the upper bound of $\Delta(\Theta_t)$ in (22). ■

APPENDIX C PROOF OF LEMMA 2

Proof: The derivation follows the same steps as the one in Lemma 3 in [12]. We provide it here briefly. Since $C(\gamma_t)$ is a continuous, convex, non-decreasing function in γ_t with $C'(\gamma_t) \geq 0$ and $C'(\gamma_t)$ increasing with γ_t . Denote the objective of $\mathbf{P4}_a$ by $J(\gamma_t)$. Since $\mathbf{P4}_a$ is convex, we examine the derivative of $J(\gamma_t)$ given by $J'(\gamma_t) = H_t + VC'(\gamma_t)$.

1) For $H_t \geq 0$: We have $J'(\gamma_t) > 0$, thus $J(\gamma_t)$ monotonically increases, with its minimum obtained at $\gamma_t^* = 0$.

2) For $H_t < -VC'(\Gamma)$: Since $VC'(\Gamma) \geq VC'(\gamma_t)$, we have $H_t + VC'(\gamma_t) < 0$. $J(\gamma_t)$ monotonically decreases, and its minimum is reached with $\gamma_t^* = \Gamma$.

3) For $-VC'(\Gamma) \leq H_t \leq 0$: In this case, γ_t^* is the root of $H_t + VC'(\gamma_t) = 0$, given by $\gamma_t^* = C'^{-1}(-\frac{H_t}{V})$. ■

APPENDIX D PROOF OF PROPOSITION 1

Proof: Removing the constant terms in (21) and from l_t in (22), and after regrouping the rest of terms, we have the objective function of $\mathbf{P4}_b$.

Determine $S_{s,t}^w$ and $S_{c,t}^w$: To determine how to use the remaining renewable $S_t - S_{w,t}$, we need to minimize the term $S_{c,t}^w(Z_t - g(H_t)) + VC_{rc} - S_{s,t}^w VP_{s,t}$ in the objective of $\mathbf{P4}_b$:

S1) If $Z_t - g(H_t) > 0$: We should maximize $S_{s,t}^w$ and minimize $S_{c,t}^w$. Thus, the remaining amount should be sold back to the grid and not stored into the battery. We have $S_{c,t}^w = 0$, and $S_{s,t}^w = \min\{S_t - S_{w,t}, U_{\max}\}$ or $S_{s,t}^w = \min\{S_t - S_{w,t} - F_{s,t}^w, U_{\max}\}$.

S2) If $Z_t - g(H_t) \leq 0$: The remaining renewable can be stored into the battery and/or sold back to the grid. To minimize the cost, if $VP_{s,t} \geq g(H_t) - Z_t$, we set $S_{c,t}^a = \min\{S_t - S_{w,t}, U_{\max}\}$, $S_{c,t}^a = \min\{S_t - S_{w,t} - S_{s,t}^w, R_{\max}\}$, i.e., first maximize the renewable sold back to the grid, then to the battery. If $VP_{s,t} < g(H_t) - Z_t$, we set $S_{c,t}^a = \min\{S_t - S_{w,t}, R_{\max}\}$, $S_{s,t}^a = \min\{S_t - S_{w,t} - S_{c,t}^w, U_{\max}\}$, i.e., first maximize the amount charged into the battery then consider the rest to be sold to the grid.

In the objective function of $\mathbf{P4}_b$, the optimal $F_{s,t}$, E_t and $S_{c,t}$ depend on the sign of $Z_t - |g(H_t)| + VP_{s,t}$, $Z_t - g(H_t) + VP_{b,t}$, and $Z_t - g(H_t)$, respectively. These three functions have the following relations: If $H_t \geq 0$,

$$Z_t - g(H_t) \leq Z_t - g(H_t) + VP_{s,t} < Z_t - g(H_t) + VP_{b,t}. \quad (40)$$

If $H_t < 0$, the following two relations are possible

$$Z_t - g(H_t) \leq Z_t - |g(H_t)| + VP_{s,t} < Z_t - g(H_t) + VP_{b,t}, \quad (41)$$

$$Z_t - |g(H_t)| + VP_{s,t} \leq Z_t - g(H_t) < Z_t - g(H_t) + VP_{b,t}. \quad (42)$$

Based on the relations in (40)–(42), we have the following five cases and derive the optimal solution in each case.

1) For $Z_t - g(H_t) + VP_{b,t} \leq 0$: From (40) and (42), to minimize the objective function of $\mathbf{P4}_b$, $F_{s,t} = 0$, and we want to maximize E_t^w . This means the battery is in the charging state. We have $1_{R,t} = 1$, $1_{D,t} = 0$, $F_{d,t}^w = F_{s,t}^w = 0$, and use maximum charging rate $S_{c,t}^w + Q_t^w = R_{\max}$ if possible. Since $Z_t - g(H_t) \leq Z_t - g(H_t) + VP_{b,t} \leq 0$, between Q_t^w and $S_{c,t}^w$, determining $S_{c,t}^w$ first will further reduce the objective value of $\mathbf{P4}_b$. Since $Z_t - g(H_t) \leq 0$, $(S_{c,t}^w, S_{s,t}^w) = (S_{c,t}^a, S_{s,t}^a)$ as in S2) given earlier. By supply-demand balancing equation (9), we obtain Q_t^w and E_t^w in (26). Alternatively, we can keep the battery idle and only buy energy E_t^{id} from the grid, where $S_{c,t}^{\text{id}} + Q_t^{\text{id}} = 0$. In this case, the battery cost can be avoided: $1_{R,t} = 1_{D,t} = 0$, but E_t^{id} will be smaller. The optimal \mathbf{a}_t^* is the one that achieves the minimum objective value.

2) For $\max\{Z_t - g(H_t), Z_t - |g(H_t)| + VP_{s,t}\} < 0 \leq Z_t - g(H_t) + VP_{b,t}$: In this case, to minimize the objective of $\mathbf{P4}_b$, we want to set E_t^w as small as possible and $F_{s,t}^w = 0$. It is possible that the battery is in either charging or discharging state. If we charge the battery, it should only be charged from renewable $S_{c,t}^w$, while $Q_t^w = 0$. Since $Z_t - g(H_t) < 0$,

$(S_{c,t}^w, S_{s,t}^w) = (S_{c,t}^a, S_{s,t}^a)$ as in S2) given earlier. Note that, if in the charging state, it means $S_{c,t}^w > 0$, which happens when $W_t = S_{w,t} < S_t$, and we have $F_{d,t}^w = 0$. Thus, constraint (6) is satisfied. On the other hand, if $W_t > S_{w,t}$, it means $S_t = S_{w,t}$ and $S_{s,t}^w = S_{c,t}^w = 0$. We could either use the battery and/or buy energy E_t^w (i.e., idle or discharging state) to serve the load. If the battery is in the discharging state, the amount $F_{d,t}^w$ should be set as large as possible to minimize E_t^w . Based on the above, we have the control solution \mathbf{a}_t^w as shown in (27). Alternatively, we can keep the battery idle to avoid battery cost, and only buy energy E_t^{id} from the grid. Thus, the optimal \mathbf{a}_t^* is chosen by whichever achieves the minimum objective value.

3) For $Z_t - g(H_t) \leq 0 \leq Z_t - |g(H_t)| + VP_{s,t}$: This is the case when (40) and (41) hold. To minimize the objective of $\mathbf{P4}_b$, one possible solution is to minimize E_t^w and maximize $F_{s,t}^w$. Due to constraint (6), $S_{c,t}^w \cdot F_{s,t}^w = 0$ must be satisfied. Thus, we have two conditions: i) If $F_{s,t}^w \geq 0$ and $S_{c,t}^w = 0$, it means the remaining amount $S_t - S_{w,t}$, if any, will be only sold back to the grid. Since $Z_t \leq g(H_t)$, it is easy to see that $0 < Z_t - |g(H_t)| + VP_{s,t} \leq VP_{s,t}$. Thus, we first maximize $S_{s,t}^w$ and then maximize $F_{s,t}^w$. Since $Z_t - g(H_t) \leq 0$, $(S_{c,t}^w, S_{s,t}^w) = (S_{c,t}^a, S_{s,t}^a)$ as in S2). The control solution \mathbf{a}_t^w is shown as in (28). ii) If $S_{c,t}^w \geq 0$ and $F_{s,t}^w = 0$, the battery will be charged from $S_{c,t}^w$ only and no energy from the battery will be sold. We have $(S_{c,t}^w, S_{s,t}^w) = (S_{c,t}^a, S_{s,t}^a)$ as in S2). The control solution \mathbf{a}_t^w is shown as in (29). After comparing i) and ii), \mathbf{a}_t^w is the one whichever achieves the less objective value. Alternatively, we can keep the battery idle. Thus, the optimal \mathbf{a}_t^* is chosen by whichever achieves the minimum objective value between \mathbf{a}_t^w and \mathbf{a}_t^{id} .

4) For $Z_t - |g(H_t)| + VP_{s,t} < 0 \leq Z_t - g(H_t)$: Note that this case happens when $H_t < 0$ and (42) holds. We want to set E_t^w as small as possible and $F_{s,t}^w = 0$. Since $Z_t \geq g(H_t)$, from earlier we have $S_{c,t}^w = 0$. Thus, the battery can be in the discharging state, and it is straightforward to obtain \mathbf{a}_t^w in (30). After comparing to the alternative idle state, the optimal \mathbf{a}_t^* is chosen by whichever achieves the minimum objective value.

5) For $\min\{Z_t - g(H_t), Z_t - |g(H_t)| + VP_{s,t}\} > 0$: Since $Z_t > g(H_t)$, $S_{c,t}^w = 0$. By (40)-(42), to minimize the objective of $\mathbf{P4}_b$, we want to minimize E_t^w and maximize $F_{s,t}^w$. This means no charging: $Q_t^w = 0$. Thus, only the discharging or idle state could be considered. For the discharging state, since $Z_t - |g(H_t)| + VP_{s,t} < Z_t - g(H_t) + VP_{b,t}$, we should first maximize the discharging amount as $F_{d,t}^w = \min\{W_t - S_{w,t}, D_{\max}\}$ to minimize E_t^w , then maximize $F_{s,t}^w$. For energy selling, between $F_{s,t}^w$ and $S_{s,t}^w$, to minimize the cost, if $Z_t - |g(H_t)| > 0$, we should first maximize $F_{s,t}^w$ from the battery and then sell from the renewable, as $F_{s,t}^w$ and $S_{s,t}^w$ in (31). Otherwise, we first sell as much as possible from the renewable, and then determine $F_{s,t}^w$ as given in (32). By supply-demand equation (9), E_t^w can be obtained as in (31) and (32). Alternatively, we can keep the battery idle and only buy energy E_t^{id} from the grid. The optimal \mathbf{a}_t^* is the one that achieves the minimum objective value.

APPENDIX E PROOF OF PROPOSITION 2

Proof: Before going into the details, we first provide an outline of our proof. Using the solutions γ_t^* and \mathbf{a}_t^* of $\mathbf{P4}_a$ and $\mathbf{P4}_b$, respectively, we can show that both Z_t and H_t are upper and lower bounded. Then, by applying these bounds to (20) and using the battery capacity constraint (7), we obtain A_o as the minimum value that can be achieved with a given value of Δ_a . With A_o obtained, we derive the upper bound of V , i.e., V_{\max} , to ensure that (7) is satisfied.

To prove Proposition 2, we first introduce Lemma 3 and Lemma 4 below.

Lemma 3: For γ_t^* in (25), H_t is bounded by

$$H_{\min} \leq H_t \leq H_{\max} \quad (43)$$

where $H_{\min} \triangleq -VC'(\Gamma) - \Gamma < 0$, and $H_{\max} \triangleq \Gamma$.

Proof:

1) *Upper bound:* From (10), $x_{u,t} \geq 0$. If $H_t \geq 0$, from (25), we have $\gamma_t^* = 0$. Thus, based on the dynamics of H_t in (19), $H_{t+1} \leq H_t$, i.e., non-increasing. When $H_t < 0$, from (25), the maximum increment of H_{t+1} in (19) is when $\gamma_t^* = \Gamma$ and $x_{u,t} = 0$, and thus $H_{t+1} \leq \Gamma = H_{\max}$.

2) *Lower bound:* From (25), if $H_t < -VC'(\Gamma)$, we have $\gamma_t^* = \Gamma$, and H_{t+1} is non-decreasing in (19). If $H_t \geq -VC'(\Gamma)$, the maximum decrement of H_{t+1} from H_t in (19) is when $\gamma_t^* = 0$ and $x_{u,t} = \Gamma$, and $H_{t+1} \geq -VC'(\Gamma) - \Gamma = H_{\min}$. Since $C(\cdot)$ is non-decreasing, $C'(\cdot) \geq 0$, we have $H_{\min} < 0$. ■

Lemma 4: Under the proposed solution in Proposition 1, we have

- 1) If $Z_t < -VP_b^{\max} + H_{\min}/\eta_d$, then $F_{d,t}^* + F_{s,t}^* = 0$;
- 2) If $Z_t > \max\{\eta_c H_{\max}, |H_{\min}|/\eta_d - VP_s^{\min}\}$, then $S_{r,t}^* + Q_t^* = 0$.

Proof: Note that $H_{\min} < 0$ and $H_{\max} > 0$. 1) This case corresponds to Case 1) in Proposition 1. We have $Z_t < -VP_b^{\max} + H_{\min}/\eta_d \leq -VP_b^{\max} + g(H_t)$, thus $F_{d,t}^* + F_{s,t}^* = 0$ is the optimal control action. 2) This case corresponds to Case 5) in Proposition 1. From Lemma 3, we know $|H_{\min}| > |H_{\max}|$. Thus, it is easy to see that if $Z_t > \max\{\eta_c H_{\max}, |H_{\min}|/\eta_d - VP_s^{\min}\}$, then $S_{c,t}^* = Q_t^* = 0$ are the optimal control action. ■

Now, we are ready to prove Proposition 2. When first show that under A_o and V in (34) and (33), B_t is always upper bounded by B_{\max} ; Then we prove that B_t is lower bounded by B_{\min} .

A. Upper Bound $B_t \leq B_{\max}$

Based on Lemma 4.1), we have $F_{d,t}^* + F_{s,t}^* = 0$ if $Z_t < -VP_b^{\max} + H_{\min}/\eta_d$, no discharging from the battery. When $Z_t \geq -VP_b^{\max} + H_{\min}/\eta_d$, from (5), the maximum decreasing amount from Z_t to Z_{t+1} in (18) in the next time slot is D_{\max}/η_d , and we have, for $t \in [0, T_o - 1]$,

$$Z_{t+1} \geq -VP_b^{\max} - \frac{\Delta_a}{T_o} - \frac{D_{\max} - H_{\min}}{\eta_d}. \quad (44)$$

In (20), we have $B_t = Z_t + A_o + \frac{\Delta_a}{T_o}t$. To satisfy the lower bound of B_t in (7), we must ensure $Z_t + A_o + \frac{\Delta_a}{T_o}t \geq B_{\min}$.

From (44), it is sufficient to let $-VP_b^{\max} - \frac{\Delta_a}{T_o} - (D_{\max} - H_{\min})/\eta_d + A_o + \frac{\Delta_a}{T_o}t \geq B_{\min}$, which means

$$A_o \geq B_{\min} + VP_b^{\max} + \frac{D_{\max} - H_{\min}}{\eta_d} + \frac{\Delta_a}{T_o}(1 - t), \quad (45)$$

for all $t \in [0, T_o]$. We next determine the minimum possible value of A_o based on the sign of Δ_a .

1) If $\Delta_a \geq 0$: The minimum value of A_o in (45) is

$$A_{o,\min} = B_{\min} + VP_b^{\max} + \frac{D_{\max} - H_{\min}}{\eta_d} + \frac{\Delta_a}{T_o}. \quad (46)$$

As a result, we have $A_t = A_{o,\min} + \frac{\Delta_a}{T_o}t$.

Based on Lemma 4.2), we have $S_{r,t}^* + Q_t^* = 0$ if $Z_t - \frac{\Delta_a}{T_o} > \max\{\eta_c H_{\max}, |H_{\min}|/\eta_d - VP_s^{\min}\} - \frac{\Delta_a}{T_o}$, i.e., no charging for the battery. When $Z_t - \frac{\Delta_a}{T_o} \leq \max\{\eta_c H_{\max}, |H_{\min}|/\eta_d - VP_s^{\min}\} - \frac{\Delta_a}{T_o}$, based on the maximum increment of Z_t to Z_{t+1} in (18), we have, for $t \in [0, T_o]$,

$$Z_t \leq \max\{\eta_c H_{\max}, \frac{|H_{\min}|}{\eta_d} - VP_s^{\min}\} - \frac{\Delta_a}{T_o} + \eta_c R_{\max}. \quad (47)$$

Substituting A_t with $A_{o,\min}$ in (46) into (20), and from (47), we have

$$B_t \leq B_{\min} + \max\{\eta_c H_{\max}, \frac{|H_{\min}|}{\eta_d} - VP_s^{\min}\} + \eta_c R_{\max} + VP_b^{\max} + \frac{D_{\max} - H_{\min}}{\eta_d} + \frac{\Delta_a}{T_o}t. \quad (48)$$

For the control solution to be feasible, we need $B_t \leq B_{\max}$. This is satisfied if RHS of (48) $\leq B_{\max}$, for all $t \in [0, T_o]$. Using H_{\min} and H_{\max} expressions in Lemma 3, this means

$$\begin{aligned} VP_b^{\max} &\leq \tilde{B}_t + \frac{H_{\min}}{\eta_d} - \max\{\eta_c H_{\max}, \frac{|H_{\min}|}{\eta_d} - VP_s^{\min}\} \\ &\leq \tilde{B}_t - \frac{VC'(\Gamma)}{\eta_d} - \Gamma\left(\frac{1}{\eta_d} + \eta_c\right) \\ &\quad - \max\{0, V\left(\frac{C'(\Gamma)}{\eta_d} - P_s^{\min}\right) + \Gamma\left(\frac{1}{\eta_d} - \eta_c\right)\} \\ &= \tilde{B}_t - \frac{VC'(\Gamma) - 2\Gamma}{\eta_d} - \max\left\{\Gamma\left(\eta_c - \frac{1}{\eta_d}\right), V\left(\frac{C'(\Gamma)}{\eta_d} - P_s^{\min}\right)\right\} \end{aligned}$$

where $\tilde{B}_t \triangleq B_{\max} - B_{\min} - \eta_c R_{\max} - D_{\max}/\eta_d - \frac{\Delta_a}{T_o}t$. To satisfy the above inequality, it is suffice that the following holds

$$VP_b^{\max} \leq \tilde{B}_t - \frac{VC'(\Gamma) - 2\Gamma}{\eta_d} - V \max\{0, \left(\frac{C'(\Gamma)}{\eta_d} - P_s^{\min}\right)\},$$

which is satisfied if $V \in (0, V_{\max}]$ with

$$V_{\max} = \frac{\tilde{B}_0 - 2\Gamma/\eta_d - \Delta_a}{P_b^{\max} + C'(\Gamma)/\eta_d + [C'(\Gamma)/\eta_d - P_s^{\min}]^+}. \quad (49)$$

2) If $\Delta_a < 0$: The minimum value of A_o in (45) is

$$A_{o,\min} = B_{\min} + VP_b^{\max} + \frac{D_{\max} - H_{\min}}{\eta_d} + \frac{\Delta_a}{T_o} - \Delta_a. \quad (50)$$

Substituting $A_{o,\min}$ in A_t , and from (20) and (47), we have

$$B_t \leq B_{\min} + \max\{\eta_c H_{\max}, \frac{|H_{\min}|}{\eta_d} - VP_s^{\min}\} + \eta_c R_{\max} + VP_b^{\max} + \frac{D_{\max} - H_{\min}}{\eta_d} - \Delta_a + \frac{\Delta_a}{T_o}t. \quad (51)$$

Again, to satisfy $B_t \leq B_{\max}$, it is suffice that RHS of (51) $\leq B_{\max}$. Using the similar analysis in the case of $\Delta_a \geq 0$, the bound is satisfied if $V \in (0, V_{\max}]$ with

$$V_{\max} = \frac{\tilde{B}_0 - 2\Gamma/\eta_d - |\Delta_a|}{P_b^{\max} + C'(\Gamma)/\eta_d + [C'(\Gamma)/\eta_d - P_s^{\min}]^+}. \quad (52)$$

Combining (49) and (52) leads to (33), and from (46) or (50), we have A_o in (34).

B. Lower Bound $B_t \geq B_{\min}$.

We now show that using $A_{o,\min}$ in (46) or (50) for $\Delta_a \geq 0$ or $\Delta_a < 0$, respectively, and $V \in (0, V_{\max}]$ with V_{\max} in (49) or (52), respectively, we have $B_t \geq B_{\min}$ for all t .

1) If $\Delta_a \geq 0$: Substitute $A_{o,\min}$ in (46) in A_t , and Z_t in (20) into (44), we have $B_{\min} + \frac{\Delta_a}{T_o}t \leq B_t$. Since $\frac{\Delta_a}{T_o}t > 0$, for $t \in [0, T_o - 1]$, $B_t \geq B_{\min}$ is satisfied for $\Delta_a \geq 0$.

2) If $\Delta_a < 0$: Substitute $A_{o,\min}$ in (50) in A_t , and Z_t in (20) into (44), we have $B_{\min} + \Delta_a\left(\frac{t}{T_o} - 1\right) \leq B_t$. Since $\Delta_a\left(\frac{t}{T_o} - 1\right) > 0$, for $t \in [0, T_o - 1]$, $B_t \geq B_{\min}$ is satisfied for $\Delta_a < 0$. ■

APPENDIX F PROOF OF THEOREM 1

Proof: A T -slot sample path Lyapunov drift is defined by $\Delta_T(\Theta_t) \triangleq L(\Theta_{t+T}) - L(\Theta_t)$. We upper bound it as follows

$$\begin{aligned} \Delta_T(\Theta_t) &= \frac{1}{2} (Z_{t+T}^2 - Z_t^2 + H_{t+T}^2 - H_t^2) \\ &= Z_t \sum_{\tau=t}^{t+T-1} \left(\eta_c(Q_\tau + S_{r,\tau}) - (F_{d,\tau} + F_{s,\tau})/\eta_d - \frac{\Delta_a}{T_o} \right) \\ &\quad + H_t \sum_{\tau=t}^{t+T-1} (\gamma_\tau - x_{u,\tau}) + \frac{1}{2} \left[\sum_{\tau=t}^{t+T-1} (\gamma_\tau - x_{u,\tau}) \right]^2 \\ &\quad + \frac{1}{2} \left[\sum_{\tau=t}^{t+T-1} \left(\eta_c(Q_\tau + S_{r,\tau}) - (F_{d,\tau} + F_{s,\tau})/\eta_d - \frac{\Delta_a}{T_o} \right) \right]^2 \\ &\leq Z_t \sum_{\tau=t}^{t+T-1} \left(\eta_c(Q_\tau + S_{r,\tau}) - (F_{d,\tau} + F_{s,\tau})/\eta_d - \frac{\Delta_a}{T_o} \right) \\ &\quad + H_t \sum_{\tau=t}^{t+T-1} (\gamma_\tau - x_{u,\tau}) + GT^2 \end{aligned} \quad (53)$$

where G is defined in Lemma 1.

Let $T_o = MT$. We consider a per-frame optimization problem below, with the objective of minimizing the time-averaged system cost within the m th frame of length T time slots.

$$\mathbf{P}_f : \min_{\{\mathbf{a}_t, \gamma_t\}} \frac{1}{T} \sum_{t=mT}^{(m+1)T-1} [E_t P_{b,t} - (F_{s,t} + S_{s,t})P_{s,t} + x_{e,t} + C(\gamma_t)]$$

s.t. (9), (1), (6), (13), (14), (17), and (16).

We show that \mathbf{P}_f is equivalent to \mathbf{P}_1 in which T_o is replaced by T . Let u_m^f denote the minimum objective value of \mathbf{P}_f . The optimal solution of \mathbf{P}_1 satisfies all constraints of \mathbf{P}_f and therefore is feasible to \mathbf{P}_f . Thus, we have $u_m^f \leq u_m^{\text{opt}}$. By

Jensen's inequality and convexity of $C(\cdot)$, we have $\overline{C(\gamma)} \geq C(\bar{\gamma}) = C(\bar{x}_u)$. Note that introducing the auxiliary variable γ_t with constraints (16) and (17) does not modify the problem. This means $u_m^f \geq u_m^{\text{opt}}$. Hence, we have $u_m^f = u_m^{\text{opt}}$ and \mathbf{P}_f and $\mathbf{P1}$ are equivalent.

From (53) and the objective of \mathbf{P}_f , we have the T -slot drift-plus-cost metric for the m th frame upper bounded by

$$\begin{aligned} & \Delta_T(\Theta_t) \\ & + V \sum_{t=mT}^{(m+1)T-1} [E_t P_{b,t} - (F_{s,t} + S_{s,t})P_{s,t} + x_{e,t} + C(\gamma_t)] \\ & \leq Z_t \sum_{t=mT}^{(m+1)T-1} \left(\eta_c(Q_\tau + S_{r,\tau}) - (F_{d,\tau} + F_{s,\tau})/\eta_d - \frac{\Delta_a}{T_o} \right) \\ & + H_t \sum_{t=mT}^{(m+1)T-1} (\gamma_t - x_{u,t}) + GT^2 \\ & + V \sum_{t=mT}^{(m+1)T-1} [E_t P_{b,t} - (F_{s,t} + S_{s,t})P_{s,t} + x_{e,t} + C(\gamma_t)]. \end{aligned} \quad (54)$$

Let $\{\tilde{\mathbf{a}}_t, \tilde{\gamma}_t\}$ denote a pair of feasible solution of \mathbf{P}_f , satisfying the following relations

$$\sum_{t=mT}^{(m+1)T-1} \eta_c (\tilde{Q}_t + \tilde{S}_{r,t}) = \sum_{t=mT}^{(m+1)T-1} \left(\frac{\tilde{F}_{d,t} + \tilde{F}_{s,t}}{\eta_d} + \frac{\Delta_a}{T_o} \right) \quad (55)$$

$$\sum_{t=mT}^{(m+1)T-1} \tilde{\gamma}_t = \sum_{t=mT}^{(m+1)T-1} \tilde{x}_{u,t} \quad (56)$$

with the corresponding objective value denoted as \tilde{u}_m^f .

Note that comparing with $\mathbf{P1}$, we impose per-frame constraints (55) and (56) as oppose to (15) and (17) for the T_o -slot period. Let $\delta \geq 0$ denote the gap of \tilde{u}_m^f to the optimal objective value u_m^{opt} , i.e., $\tilde{u}_m^f = u_m^{\text{opt}} + \delta$.

Among all feasible control solutions satisfying (55) and (56), there exists a solution which leads to $\delta \rightarrow 0$. The upper bound in (54) can be rewritten as

$$\begin{aligned} & \Delta_T(\Theta_t) + V \sum_{t=mT}^{(m+1)T-1} [E_t P_{b,t} - (F_{s,t} + S_{s,t})P_{s,t} + x_{e,t} + C(\gamma_t)] \\ & \leq GT^2 + VT \lim_{\delta \rightarrow 0} (u_m^{\text{opt}} + \delta) = GT^2 + VT u_m^{\text{opt}}. \end{aligned} \quad (57)$$

Summing both sides of (57) over m for $m = 0, \dots, M-1$, and dividing them by VMT , we have

$$\begin{aligned} & \frac{L(\Theta_{T_o}) - L(\Theta_0)}{VMT} \\ & + \frac{1}{MT} \sum_{m=0}^{M-1} \sum_{t=mT}^{(m+1)T-1} [E_t P_{b,t} - (F_{s,t} + S_{s,t})P_{s,t} + x_{e,t} + C(\gamma_t)] \\ & \leq \frac{1}{M} \sum_{m=0}^{M-1} u_m^{\text{opt}} + \frac{GT}{V}. \end{aligned} \quad (58)$$

Since $\overline{C(\gamma)} \geq C(\bar{\gamma})$ for the convex function $C(\cdot)$ where $\bar{\gamma} \triangleq \frac{1}{T_o} \sum_{t=0}^{T_o-1} \gamma_t$, from (58), we have

$$\frac{1}{T_o} \sum_{t=0}^{T_o-1} [E_t P_{b,t} - (F_{s,t} + S_{s,t})P_{s,t}] + \bar{x}_e + C(\bar{\gamma})$$

$$\leq \frac{1}{T_o} \sum_{t=0}^{T_o-1} [E_t P_{b,t} - (F_{s,t} + S_{s,t})P_{s,t} + x_{e,t} + C(\gamma_t)]. \quad (59)$$

For a continuously differentiable convex function $f(\cdot)$, the following inequality holds [33]

$$f(x) \geq f(y) + f'(y)(x - y). \quad (60)$$

Applying (60) to $C(\bar{x}_u)$ and $C(\bar{\gamma})$, we have

$$\begin{aligned} C(\bar{x}_u) & \leq C(\bar{\gamma}) + C'(\bar{x}_u)(\bar{x}_u - \bar{\gamma}) \leq C(\bar{\gamma}) + C'(\Gamma)(\bar{x}_u - \bar{\gamma}) \\ & = C(\bar{\gamma}) - C'(\Gamma) \frac{H_{T_o} - H_0}{T_o} \end{aligned} \quad (61)$$

where the last term in (61) is obtained by summing both sides of (19) over T_o .

Applying the inequality (61) to $C(\bar{\gamma})$ at the LHS of (59), and further applying the inequality (59) to the LHS of (58), we have the bound of the objective value $u^*(V)$ of $\mathbf{P1}$ achieved by Algorithm 1 as in (35).

For the bound in (35), note that H_t is bounded as in (43), and Z_t is bounded by (44) and (47). It follows that $L(\Theta_t)$ is bounded. As $T_o \rightarrow \infty$, we have $\frac{C'(\Gamma)(H_0 - H_{T_o})}{T_o} \rightarrow 0$ and $\frac{L(\Theta_0) - L(\Theta_{T_o})}{VT_o} \rightarrow 0$, and (36) follows. ■

APPENDIX G

PROOF OF PROPOSITION 3

Proof: For $t = T_o$, from the dynamic shifting in (20), we have $Z_{T_o} = B_{T_o} - A_o - \Delta_a$. For $t = 0$, we have $Z_0 = B_0 - A_o$. Thus, we have the following relation: $\frac{1}{T_o}(Z_{T_o} - Z_0) = \frac{1}{T_o}(B_{T_o} - B_0) - \frac{\Delta_a}{T_o}$. Substituting the first equation in (15) into the above, we have

$$\frac{Z_{T_o} - Z_0}{T_o} = \frac{\sum_{\tau=0}^{T_o-1} [\eta_c(Q_\tau + S_{r,\tau}) - \frac{F_{d,\tau} + F_{s,\tau}}{\eta_d}] - \Delta_a}{T_o}.$$

Note that Z_t in (18) is derived from the above. Since this finite time horizon algorithm, (15) is satisfied with error $\epsilon = Z_{T_o} - Z_0$. Because Z_t is bounded by (44) and (47) and H_t is bounded by (43), the error ϵ has the following upper bound

$$\begin{aligned} |\epsilon| & \leq \max\{\eta_c H_{\max}, |H_{\min}|/\eta_d - VP_s^{\min}\} + \eta_c R_{\max} \\ & + VP_b^{\max} - H_{\min}/\eta_d + D_{\max}/\eta_d \\ & \leq \max\{H_{\max}/\eta_d + |H_{\min}|/\eta_d, 2|H_{\min}|/\eta_d - VP_s^{\min}\} \\ & + VP_b^{\max} + \eta_c R_{\max} + D_{\max}/\eta_d \\ & = (2\Gamma + VC'(\Gamma))/\eta_d + \max\{0, VC'(\Gamma)/\eta_d - VP_s^{\min}\} \\ & + VP_b^{\max} + \eta_c R_{\max} + D_{\max}/\eta_d. \end{aligned} \quad (62)$$

Thus, we complete the proof. ■

APPENDIX H

PROOF OF PROPOSITION 4

Proof: To ensure (3) is satisfied, we must show the optimal control solution (26)-(30) in Proposition 1 can ensure (3) being satisfied. For Cases 1, 2 and 4, from their optimal control solutions (26), (27) and (30), it is easy to see that (3) is satisfied. For Cases 3 and 5, from their optimal control solutions (31) or (32) and (28) or (29), if $F_{d,t}^w = W_t - S_{w,t} < D_{\max}$, $E_t^w = 0$ and $F_{s,t} \geq 0$; If $F_{d,t}^w = D_{\max}$, we have $F_{s,t}^w = 0$ and $E_t^w \geq 0$. If the battery is in the idle state, we always have $F_{s,t}^{\text{id}} = 0$. Thus, (3) is a sufficient condition for Algorithm 1. ■

REFERENCES

- [1] P. Denholm, E. Ela, B. Kirby, and M. Milligan, "The role of energy storage with renewable electricity generation," National Renewable Energy Laboratory, Tech. Rep. NREL/TP-6A2-47187, Jan. 2010.
- [2] A. Castillo and D. F. Gayme, "Grid-scale energy storage applications in renewable energy integration: A survey," *Energy Convers. Manage.*, vol. 87, pp. 885–894, Nov. 2014.
- [3] H.-I. Su and A. El Gamal, "Modeling and analysis of the role of energy storage for renewable integration: Power balancing," *IEEE Trans. Power Syst.*, vol. 28, pp. 4109–4117, Nov. 2013.
- [4] S. Sun, M. Dong, and B. Liang, "Real-time power balancing in electric grids with distributed storage," *IEEE J. Select. Topics Signal Processing*, vol. 8, pp. 1167–1181, Dec. 2014.
- [5] S. Sun, B. Liang, M. Dong, and J. A. Taylor, "Phase balancing using energy storage in power grids under uncertainty," *IEEE Trans. Power Syst.*, vol. 31, no. 5, pp. 3891–3903, Sep. 2016.
- [6] S. Sun, M. Dong, and B. Liang, "Distributed real-time power balancing in renewable-integrated power grids with storage and flexible loads," *IEEE Trans. Smart Grid*, vol. 7, no. 5, pp. 2337–2349, Sep. 2016.
- [7] Y. Zhang, N. Gatsis, and G. Giannakis, "Robust energy management for microgrids with high-penetration renewables," *IEEE Trans. Sustain. Energy*, vol. 4, pp. 944–953, Oct 2013.
- [8] A. Faruqui, R. Hledik, and J. Tsoukalis, "The power of dynamic pricing," *Electr. J.*, vol. 22, no. 3, pp. 42–56, 2009.
- [9] C. Joe-Wong, S. Sen, S. Ha, and M. Chiang, "Optimized day-ahead pricing for smart grids with device-specific scheduling flexibility," *IEEE J. Sel. Areas Commun.*, vol. 30, pp. 1075–1085, Jul. 2012.
- [10] Y. Wang, X. Lin, and M. Pedram, "Adaptive control for energy storage systems in households with photovoltaic modules," *IEEE Trans. Smart Grid*, vol. 5, no. 2, pp. 992–1001, Mar. 2014.
- [11] M. He, S. Murugesan, and J. Zhang, "A multi-timescale scheduling approach for stochastic reliability in smart grids with wind generation and opportunistic demand," *IEEE Trans. Smart Grid*, vol. 4, pp. 521–529, Mar. 2013.
- [12] T. Li and M. Dong, "Real-time energy storage management with renewable integration: Finite-time horizon approach," *IEEE J. Sel. Areas Commun.*, vol. 33, no. 12, pp. 2524–2539, Dec. 2015.
- [13] —, "Real-time residential-side joint energy storage management and load scheduling with renewable integration," *IEEE Trans. Smart Grid*, vol. 9, pp. 283–298, Jan. 2018.
- [14] Y. Zhang and M. van der Schaar, "Structure-aware stochastic storage management in smart grids," *IEEE J. Sel. Topics Signal Process.*, vol. 8, pp. 1098–1110, Dec. 2014.
- [15] M. R. V. Moghadam, R. Zhang, and R. T. B. Ma, "Demand response for contingency management via real-time pricing in smart grids," in *Proc. IEEE Int. Conf. Smart Grid Commun. (SmartGridComm)*, Nov. 2014, pp. 632–637.
- [16] T. Ackermann, G. Andersson, and L. Söder, "Overview of government and market driven programs for the promotion of renewable power generation," *Renewable Energy*, vol. 22, no. 1-3, pp. 197–204, 2001.
- [17] R. Uргаonkar, B. Uргаonkar, M. J. Neely, and A. Sivasubramaniam, "Optimal power cost management using stored energy in data centers," in *Proc. ACM SIGMETRICS*, Jun. 2011.
- [18] K. Rahbar, J. Xu, and R. Zhang, "Real-time energy storage management for renewable integration in microgrid: An off-line optimization approach," *IEEE Trans. Smart Grid*, vol. 6, pp. 124–134, Jan 2015.
- [19] L. Huang, J. Walrand, and K. Ramchandran, "Optimal demand response with energy storage management," in *Proc. IEEE SmartGridComm*, 2012.
- [20] S. Salinas, M. Li, P. Li, and Y. Fu, "Dynamic energy management for the smart grid with distributed energy resources," *IEEE Trans. Smart Grid*, vol. 4, pp. 2139–2151, Sep. 2013.
- [21] T. Li and M. Dong, "Online control for energy storage management with renewable energy integration," in *Proc. IEEE Int. Conf. Acoust. Speech Signal Process. (ICASSP)*, May 2013.
- [22] —, "Real-time energy storage management with renewable energy of arbitrary generation dynamics," in *Proc. Asilomar Conf. Signals Syst. Comput.*, Nov. 2013.
- [23] —, "Real-time energy storage management: Finite-time horizon approach," in *Proc. IEEE Int. Conf. Smart Grid Commun. (SmartGridComm)*, Nov. 2014, pp. 115–120.
- [24] J. Qin, Y. Chow, J. Yang, and R. Rajagopal, "Distributed online modified greedy algorithm for networked storage operation under uncertainty," *IEEE Trans. Smart Grid*, vol. 7, no. 2, pp. 1106–1118, Mar. 2016.
- [25] M. J. Neely, *Stochastic Network Optimization with Application to Communication and Queuing Systems*. Morgan & Claypool, 2010.
- [26] B. G. Kim, S. Ren, M. van der Schaar, and J. W. Lee, "Bidirectional energy trading and residential load scheduling with electric vehicles in the smart grid," *IEEE J. Sel. Areas Commun.*, vol. 31, no. 7, pp. 1219–1234, Jul. 2013.
- [27] C. Mediawaththe, E. Stephens, D. Smith, and A. Mahanti, "Competitive energy trading framework for demand-side management in neighborhood area networks," *IEEE Trans. Smart Grid*, 2017.
- [28] Y. Huang, S. Mao, and R. Nelms, "Adaptive electricity scheduling in microgrids," *IEEE Trans. Smart Grid*, vol. 5, pp. 270–281, Jan. 2014.
- [29] P. Ramadass, B. Haran, R. White, and B. N. Popov, "Performance study of commercial LiCoO₂ and spinel-based Li-ion cells," *J. Power Sources*, vol. 111, pp. 210–220, Sep. 2002.
- [30] Y. Shi, B. Xu, Y. Tan, and B. Zhang, "A convex cycle-based degradation model for battery energy storage planning and operation," arXiv:1703.07968, Tech. Rep., Mar. 2017. [Online]. Available: <https://arxiv.org/abs/1703.07968>.
- [31] M. J. Neely, "Universal scheduling for networks with arbitrary traffic, channels, and mobility," arXiv:1001.0960, Tech. Rep., Jan. 2010. [Online]. Available: <https://arxiv.org/abs/1001.0960>.
- [32] "Electricity prices," Ontario Energy Board, 2012. [Online]. Available: <http://www.ontarioenergyboard.ca/OEB/Consumers/Electricity>
- [33] S. Boyd and L. Vandenberghe, *Convex Optimization*. Cambridge University Press, 2004.